Electrospinning and Superhydrophobic Materials

Philip Klein
Bruce Kaye
Paul Saville

DRDC - Atlantic Research Centre

Defence Research and Development Canada

Scientific Report
DRDC-RDDC-2015-R049
April 2015

Electrospinning and Superhydrophobic Materials

Philip Klein
Bruce Kaye
Paul Saville

DRDC - Atlantic Research Centre

Defence Research and Development Canada

Scientific Report
DRDC-RDDC-2015-R049
April 2015

IMPORTANT INFORMATIVE STATEMENTS

This work was sponsored through the DRDC Technology Investment Fund and was part of the DRDC Army Client Group Program.

Abstract

Many processes are affected by the interaction of liquids with surfaces. These interactions depend on the solid-liquid, solid-vapour, and liquid-vapour surface tensions, as well as the surface structure or roughness. A liquid in intimate contact with a rough surface will generally be better adhered than the same liquid on a smooth surface due to the increase in the contact area. Rough superhydrophobic surfaces with low surface energy, however, support the liquid on the peaks of the roughness, with minimal contact area, and as a consequence the liquid is easily removed. In this work durable micron sized polyurethane fibres were produced by electrospinning. The surface of these fibre mats was microscopically rough, and nano-scale features were added to the fibre surface by electrospinning with nanoparticles, or through a fluorinated alkyl silane, sol-gel coating process. The sol-gel treatment produced a rough hydrophobic coating on the electrospun fibres. From contact angle measurements, it was found that these methods increased the water contact angle, however, a truly superhydrophobic surface with small tilt angle was only achieved when a thicker sol-gel coating was deposited on the electrospun fibre mats.

Significance to defence and security

Many military systems are impacted by solid-liquid contact, whether it is contamination by chemical agents, corrosion, ice-accumulation, biofouling, degraded antenna performance, dirt accumulation and staining, or discomfort from being wet. Superhydrophobic or oleophobic materials have chemical and structural properties which limits liquid contact and wetting, permitting the liquids to be easily shed. The electrospinning of fibres is one method of producing materials with the required properties and may be applicable to oil-water separation, water proofing membranes and better rain wear.

Résumé

De nombreux processus sont affectés par l'interaction des liquides avec les surfaces. Ces interactions dépendent des tensions superficielles solide-liquide, solide-vapeur et liquide-vapeur, ainsi que de la structure de la surface et de sa rugosité. Un liquide en contact étroit avec une surface rugueuse y adhèrera généralement mieux que sur une surface lisse en raison de la surface de contact plus grande. Toutefois, les surfaces rugueuses superhydrophobes à faible énergie superficielle supportent le liquide sur leurs parties les plus rugueuses, là où le contact est minimal, et, en conséquence, le liquide facilement extrait. Pour le présent travail, nous avons produit des fibres de polyuréthane durable de la taille de l'ordre du micron par électrofilage. La surface de ces mats fibreux était rugueuse au microscope et des caractéristiques à l'échelle nanométrique ont été ajoutées à la surface des fibres par électrofilage au moyen de nanoparticules ou grâce à un procédé de revêtement sol-gel avec un alkylsilane fluoré. Le traitement par sol-gel a produit un revêtement rugueux hydrophobe sur les fibres électrofilées. À partir de mesures d'angles de contact, nous avons montré que ces méthodes accroissaient l'angle de contact de l'eau. Toutefois, seule une surface vraiment superhydrophobe avec un petit angle d'inclinaison a pu être obtenue quand un revêtement sol-gel plus épais était déposé sur les mats fibreux électrofilés.

Importance pour la défense et la sécurité

De nombreux systèmes militaires sont soumis à un contact solide-liquide, que ce soit la contamination par agents chimiques, la corrosion, l'accumulation de glace, l'encrassement biologique, la performance d'antenne dégradée, l'accumulation de poussière ou de taches ou l'inconfort dû au fait d'être mouillé. Les matières superhydrophobes ou oléophobes ont des propriétés chimiques et structurelles qui limitent le contact du liquide et le mouillage, permettant aux liquides de s'écouler facilement. L'électrofilage de fibres est une méthode permettant de produire des matières aux propriétés requises et pouvant être appliquées à la séparation huile-eau, à des membranes d'étanchéité et à de meilleurs vêtements de pluie.

Table of contents

List of figures

List of tables

This page intentionally left blank.

1 Introduction

The ability of a liquid to wet and adhere to, or to be shed from a solid surface is relevant to many military applications such as anti-biofouling coatings for boats, self-cleaning surfaces and windows, water-shedding antennas, stain-resistant textiles, water-proof clothing, and separation of oil and water.[1] Superhydrophobic surfaces have sparked interest because of the potential for creating materials that readily shed water. Nature supplies many examples of superhydrophobic surfaces such as the lotus leaf which sheds water. The ability to shed the water relies on rough protrusions from the surface that are coated with nanocrystals of a waxy material. The waxy material reduces the solid-liquid surface tension, and provides a second order of roughness. The combined nano and micron scale roughness act to minimize the contact area with water. As a result water drops can rest on top of the protrusions in a beaded state with minimal contact. If the surface is inclined, then small gravitational forces are large enough to cause the liquid to detach and roll from the surface. A variety of methods have been developed to produce superhydrophobic surfaces including template and lithographic approaches, micromachining, plasma treatments,[2,3] chemical derivatization,[4] electrochemical deposition,[5] colloidal assembly,[6] sol-gel[7-11] and electrospinning[12-14] or a combination of the techniques.[1]

In this study superhydrophobic surfaces were produced by electrospinning mats of micron and sub-micron sized fibres. Electrospun fibres have previously been shown to be capable of producing the superhydrophobic effect[14] through: the addition of nanoparticles to the electrospinning solution;[12] by electrospinning low surface energy polymers;[15] use of microphase separation;[13] or through the use of sol-gels.[16] These reports do not usually contain enough information to be able to easily reproduce the results or to apply them to other polymer or chemical systems. Hence, the electrospinning parameter space was investigated in order to determine the effect of various experimental conditions on the morphology of durable, electrospun polyurethane fibres. Nanoparticles and sol-gel coatings were used to increase the electrospun fibre roughness. The fluorinated alkyl silanes used in the sol-gel treatment acted to decrease the solid-liquid surface tension. Scanning electron microscopy, Scanning Electron Microscope (SEM), was used to determine the characteristics of the fibre and mat, and contact and tilt angle measurements were made to determine the hydrophobicity of the materials.

This work was undertaken as part of a technology investment project, investigating the use of superhydrophobic and organophobic materials for military application, for the Canadian Army Forces.

1.1 Theory

The solid-gas, solid-liquid, and liquid-gas surface tensions (γsv, γsl, γlv, respectively) acting on a liquid drop resting in equilibrium on a surface are related by the Young equation and the contact angle, the angle between the liquid-vapour and solid-liquid surface tensions, Equation 1 and Figure 1. The contact angle is indicative of whether a surface is hydrophilic, < 90°, or hydrophobic, > 90°. A liquid completely suspended on air would have a ciontact angle of 180°.[1]

$$\gamma_{SG} = \gamma_{SL} + \gamma_{LG} \cos \theta \quad (1)$$

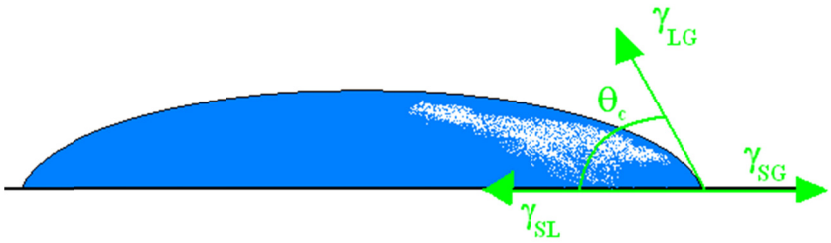

Figure 1: *Representation of a water droplet on a solid surface surrounded by air described by the Young's equation.*

Two states can exist when a liquid is in contact with a rough surface: the Wenzel and Cassie-Baxter states, Figure 2. In the Wenzel state, the liquid completely wets the solid forming a conformal interface. The measured, or apparent contact angle for a Wenzel surface, θ_w, is greater than for a smooth surface due to the increase in contact area, r. The apparent contact angle is given by

$$\cos \theta_w = r \cos \theta \tag{2}$$

In the Cassie-Baxter state the liquid is supported on the surface roughness with air trapped under it. If the surface is hydrophilic or pressure forces the air out from under the water drop, the Cassie-Baxter state will be meta-stable and can collapse to the Wenzel state, Figure 2. The contact angle for the Cassie-Baxter state, θ_c, is dependent on the fraction of the area under the drop that is in contact with the substrate, f, and $1-f$, is the area under the drop that is in contact with air.

$$\cos \theta_c = f (1 + \cos \theta) - 1 \tag{3}$$

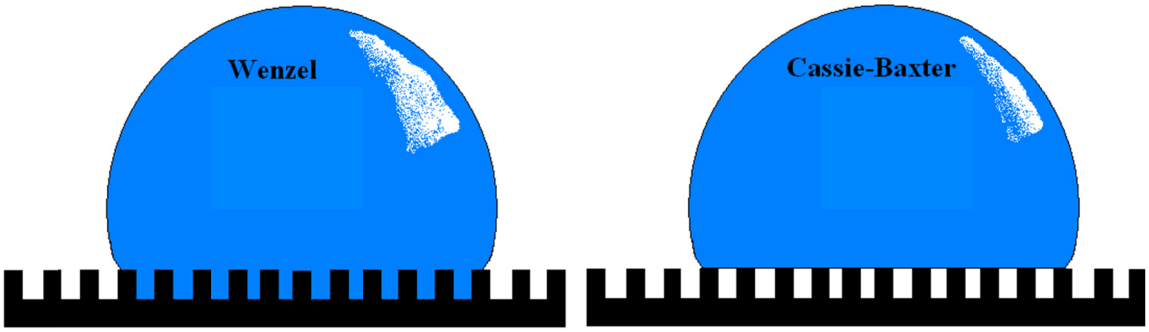

Figure 2: *Illustration of a water droplet sitting on a rough surface in each of the Wenzel and Cassie-Baxter states.*

A superhydrophobic surface is usually defined as a surface with a contact angle greater than 150^o and a tilt angle, the angle of surface tilt at which a drop will roll, which is less than 10^o, or with

small contact angle hysteresis.[12] Contact angle hysteresis is the difference between advancing and receding contact angles, which can be measured on the downhill and uphill sides of a drop on an inclined surface before the drop rolls. It can also be determined by growing or reducing the drop size.

Achieving a superhydrophobic state requires two main surface characteristics: high surface roughness to minimize the solid-liquid contact area, and low surface energy to minimize the solid-liquid surface tension. The surface tension depends on the chemical nature of the surface materials,[3] and their associated strong dipole-dipole and hydrogen bonding interactions or weaker Van der Waals forces. Low solid-liquid surface tension is often achieved between water and alkyl hydrocarbons, or fluorinated molecules, and results in the water beading due to the large liquid-air surface tension. Changing the material of the surface or applying a coating are two ways of modifying the solid-liquid surface tension.

Naturally occurring superhydrophobic materials such as the lotus leaf have micro- and nano-structures. Man-made materials with roughness on two scales can be prepared by adding nanoparticles to a surface that already contains a micron-sized roughness, or by preparing micron-sized particles from nanoparticles, and coating the surface with these.[17]

1.2 Electrospinning

Electrospinning is the technique employed to prepare fine fibres by applying a large electrical potential to a polymer solution in a syringe. The accumulation of charge on the drop's surface causes repulsive forces to develop which distort the drop's shape into a cone. This is referred to as the Taylor cone. If the repulsive electrostatic forces exceed the surface tension, a liquid jet will be ejected from the drop. This jet then travels from the syringe needle to a collector, Figure 3.[18] The jet remains stable for a short distance, termed the rectilinear region, until the electrostatic forces, and solvent evaporation, result in instabilities that cause the jet to bend. This bending is contained within the region called the envelope cone which increases in size with the distance travelled until the fibre hits the collector. The bending instability, or whipping motion, causes a massive increase in the path length the fibres travel and also stretches the fibre down to micro and sub-micron diameters. Different needle sources such as a coaxial spinneret, gas jackets, bi-component spinneret, and multiple spikes methods have been used to direct the flow of the polymer solution, and similarly different methods exist to accelerate and collect the electrospun fibres, providing scope to tailor the fibre characteristics.[19]

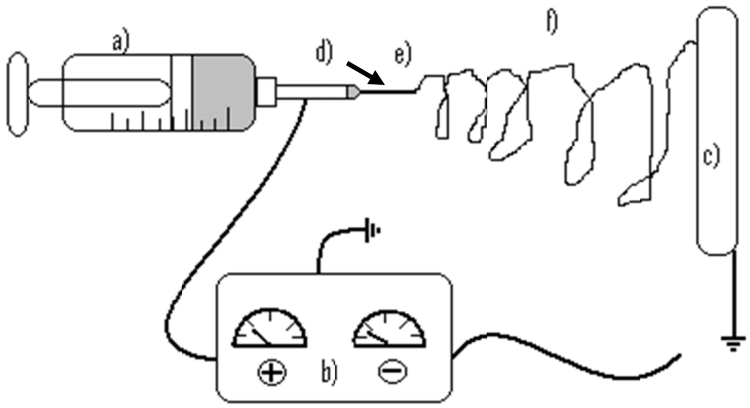

Figure 3: *(a) Example of electrospinning apparatus including syringe, (b) high voltage power supply, (c) collector, and (d) electrospinning regions include Taylor cone, (e) rectilinear and (f) envelope cone.*

For superhydrophobic material applications, electrospun fibres were collected as randomly oriented non-woven mats providing a rough surface. Control of the fibre morphology and chemical composition will determine the material's hydrophobic qualities. In addition to the formation of smooth fibres, other structures have been observed as a result of electrospinning, including beads and pores.[18] The production of beads has been achieved using low molecular weight polymers, or low polymer concentrations, while pores can result if electrospinning occurs in high humidity.[20,21] Rough fibre surfaces have been produced by adding nanoparticles to the polymer solution[12] or through chemical or coating derivatization such as by using a sol-gel process.[22]

1.3 Sol-gel

In this study, sol-gel coatings were used to produce hydrophobic surfaces with nanoscale roughness. This was accomplished by preparing a chemical precursor solution, sol, which contained nanoparticles. The substrate was dipped into, or sprayed with the sol, and left to dry.[23] As the sol dried, the nanoparticles coated the surface and reacted to form an integrated network, gel. The sol-gel system used in this study consists of tetraethoxy orthosilicate (TEOS), and a fluorinated silicate, triethoxy (3,3,4,4,5,5,6,6,7,7,8,8,8-tridecafluorooctyl) silane, tridecafluorooctyl triethoxy Silane (FAS).[24] Hydrolysis and condensation reactions occur when TEOS and FAS react to form silicate cores that are terminated by a corona of fluorinated alkyl chains, with particle diameters of about 50 nm.[24] These particles have been shown to adhere well to most textiles, and are stable to light, heat, chemical, and microbial attack.

2 Experimental

All solutions in this study were prepared on a percent weight/volume basis, whereby the components of interest were added to a volumetric flask, dissolved in solvent and made up to the mark. Solutions for electrospinning were prepared by dissolving a polyurethane resin, Pellethane (Dow Pellethane 2103-70A), in mixtures of tetrahydrofuran (THF), and N,N'-dimethyl formamide (DMF), from Sigma-Aldrich. The Pellethane is a polyurethane made from 4,4-methylene diphenyl diisocyanate, 1,4-butanediol, and polytetramethylene glycol. Polymer solutions of concentrations 5, 7.5, 10, 15, and 20% w/v Pellethane were prepared. The effect of the solvent mixture ratio, THF:DMF, was assessed using 10% w/v Pellethane solutions in solvent ratios of 100:0, 90:10, 70:30, 60:40 and 50:50, THF to DMF. Solution viscosities were measured using #3 and #6 Zeitfuchs cross arm viscometers, Cannon Instruments, with viscosity constants of 0.155 and 1.08 mm^2s^{-2}, respectively. The viscometers were used according to the manufacturer's specifications. Three measurements were made for each solution. The measurements were conducting within the electrospinning enclosure before spinning so as to capture the representative conditions. The temperature, typically 23 ± 1^{o} C, and the humidity were recorded.

A custom built acrylic enclosure fitted with an adjustable collector and several openings for needles, electrical leads, and operator access was used for electrospinning. Electrospinning was evaluated in vertical and horizontal configurations using gravity feed or a syringe pump, Cole Parmer Instrument Company SYRINGE PMP CMPTCT 115 V Model #75900-00, Figure 4. Teflon tubing with inner diameters of 3/16", and nickel plated brass single barb Luer lock fittings, McMaster-Carr, were used for connecting needle and syringe. Electrospinning was observed with the aid of a strobe light. Variables assessed included: polymer concentration, solvent composition, needle gauge, needle voltage, collector distance, and collector voltage. Each of the electrospun samples was left on the aluminum foil collector for scanning electron microscope, SEM, characterization after being carbon sputter coated. SEM images were analyzed for fibre morphology, diameter, fusing between fibres, texture, fibre shape, and mat consistency. The degree of fusing was qualitatively based on the observed range. For some of the thicker and denser mats a gold sputter coater was used in order to reduce charging during imaging.

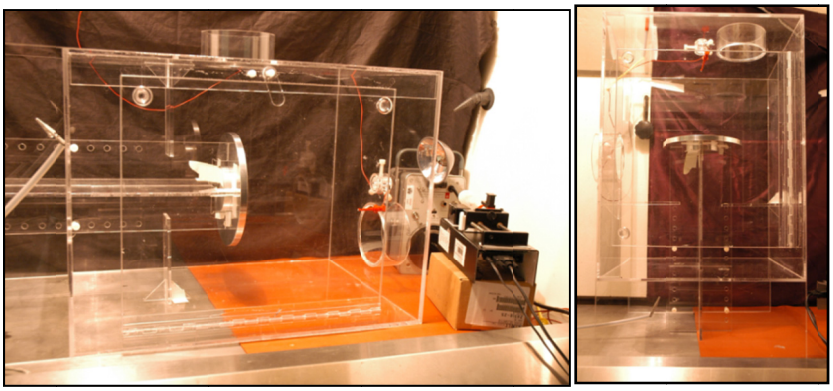

Figure 4: *Electrospinning enclosure in the horizontal (left) and vertical (right) orientations. The collector is about 25 cm from the needle tip. A strobe light and syringe pump are visible in the image on the left. An orange rubber sheet was used to insulate the syringe pump from the grounded fume hood work surface.*

2.1 Contact and tilt angle measurements

In order to assess the hydrophobic properties of the electrospun fibres, 5 μL water drops were placed at various locations on the mats still supported on the aluminum foil collector, and the contact and tilt angles measured. For mats where the electrospun fibres had visibly fused together, the contact angles were determined in regions representative of the majority of the mat's surface. Drops were imaged using a Keyence Digital microscope, Figure 5. Contact angles were measured using the microscope's image processing software. Reported contact angle measurements are an average from four water drops on the surface.

Tilt angles at which water drops rolled from the surface were measured using a machinist's vice capable of tilting up to 47^{o} from the horizontal, Figure 6. In some cases, tilt angles could not be measured due to the drops being pinned to, or stuck on the surface. Reported tilt angles are an average from five independent measurements.

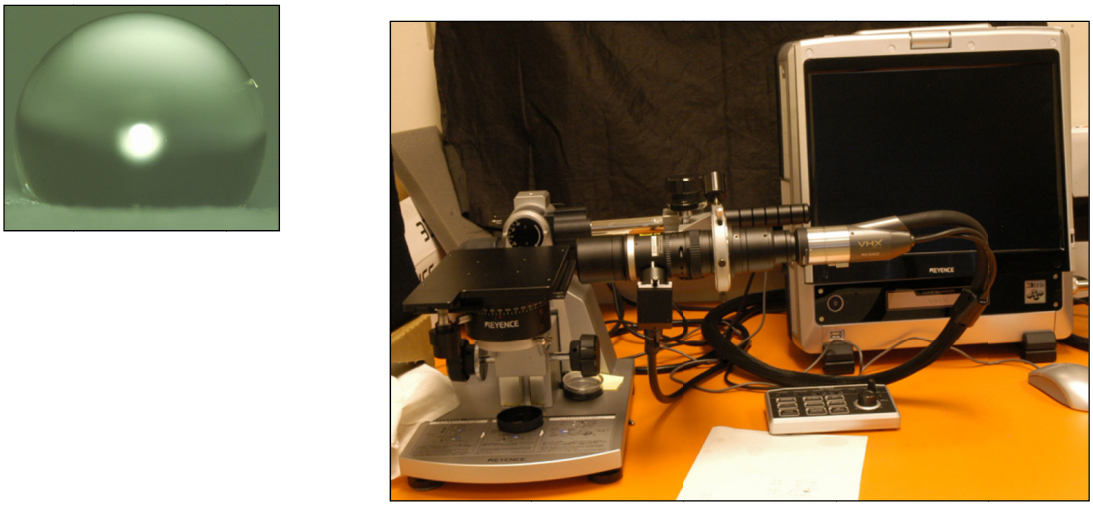

Figure 5: *The contact angle measurement apparatus. The Keyence Digital Microscope oriented at nearly 90° to the sample stage. The image in the top left shows a 5 µL water droplet at 100x magnification captured with the microscope shown.*

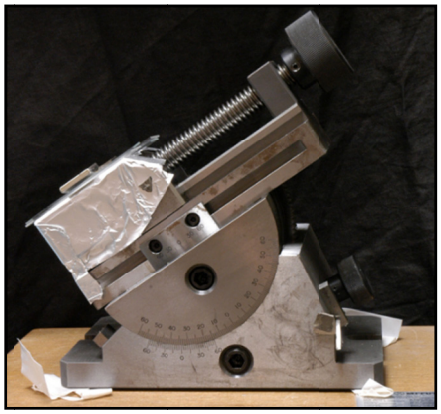

Figure 6: *Apparatus for tilt angle measurement.*

2.2 Fibre modification: nanoparticles and sol-gels

The effect of secondary roughness was studied by introducing titanium dioxide, TiO_2, nanoparticles into the electrospinning solutions. The TiO_2 used was from a source of unlabeled paint pigment. SEM imaging was used to determine that the average pigment particle diameter was 100 nm. Four solutions were prepared with two solutions containing 5 g and two solutions containing 10 g Pellethane per 100 mL total volume. Each of these solutions contained either 1g or 5 g of titanium dioxide per 100 mL of total solution volume, as well.

Electrospun fibre mats were also derivatized with rough, low surface energy particles by dipping the electrospun fibre mats into a sol-gel solution. The sol-gel mixture was prepared as follows: to 25 mL ethanol was added 0.859 mL of triethoxy (3,3,4,4,5,5,6,6,7,7,8,8,8-tridecafluorooctyl) silane, (FAS), Evonik Dynasylan F 8261, and 5 mL tetraethyl orthosilicate Sigma-Aldrich, in a 1:10 mole ratio.[24] A second solution was prepared by adding 6 mL of 28% ammonium hydroxide

to 25 mL ethanol. This solution was added to the silicate solution and stirred for approximately 18 hours before use. The sol-gel solution was sonicated prior to coating the various substrates by dipping them directly into the solution, and allowing them to air dry, followed by one hour curing at 110^{o}C.

Different substrates were coated with the sol-gel including textiles (thin and thick polyethylene terephthalate (PET) fabric, cotton, and glass fibres), electrospun fibre mats (beaded Pellethane fibres, thin Pellethane electrospun fibres, thick Pellethane electrospun fibres), spin coated Pellethane samples, and glass slides.

3 Results and discussion

3.1 Electrospinning

Initially the electrospinning apparatus was set up in the vertical orientation with gravity feed of the electrospinning solution. In this orientation, the collector – needle tip distance was limited to a maximum of 20 cm. Any solution dripping from the needle landed on the collector. The gravity feed method was sufficient for electrospinning but made comparison of the resultant fibres challenging due to the decrease in flow rate as the experiment progressed. The introduction of a programmable syringe pump resulted in better control of the flow. The syringe pump also permitted use of the apparatus in the horizontal position, eliminating the impact of drips falling onto the collector. In the horizontal configuration the needle-collector distance could be extended to 35 cm. Some electrical arcing observed at the syringe pump was addressed by coating all the bare metal portions of the pump with a few coats of acrylic paint, and by the use of Teflon sheeting between the syringe holder and base.

3.1.1 Effect of the applied potential

The potential between the needle and collector is an important factor in the electrospinning process. It is involved in the formation of the Taylor cone, the rate at which solution is ejected, and the length of the rectilinear region. Stable electrospinning conditions were determined by observation of the Taylor cone and rectilinear region. Optimum electrospinning conditions occurred when a positive potential was applied to the needle. The potential was then adjusted in order to maintain a symmetrical Taylor cone of constant size, and a rectilinear region with good trajectory and stability. If the potential was too high, then the Taylor cone and rectilinear regions were unstable and moved around very rapidly appearing to form multiple jets from the Taylor cone. If the potential was too high for the solution flow rate, the solution in the Taylor cone was depleted and would retreat into the needle. When this occurred the electrospinning would pulse rather than proceed as a steady stream. If the potential on the needle was too low for the solution flow rate, the Taylor cone extended and the liquid drop would detach from the needle (drip) when the liquid became too heavy. It was found that the electrospinning would often stabilize if the potential was set towards the high end, compared to being set too low where drop growth at the end of the needle distorted the Taylor cone.

During electrospinning, the ejected polymer solution and subsequent fibre are subject to the effects of gravity. In the horizontal orientation with the collector grounded to earth, the fibres deposited toward the lower edge of the collector plate. Application of a negative potential to the collector caused the fibres to deposit in the centre, with a reduction in the diameter of the fibre mat, Figure 7. In addition to a smaller diameter mat, there was an increase in fibre fusing. Due to the decrease in fibre transit time from the needle to collector, the solvent had not fully evaporated and wet fibres were being collected. Fusing is discussed in more detail below. The amount of fibre fusing could be reduced by decreasing the potential applied to the collector.

The two parameters which were observed to affect the potential required for optimum electrospinning results were the polymer concentration and flow rate.

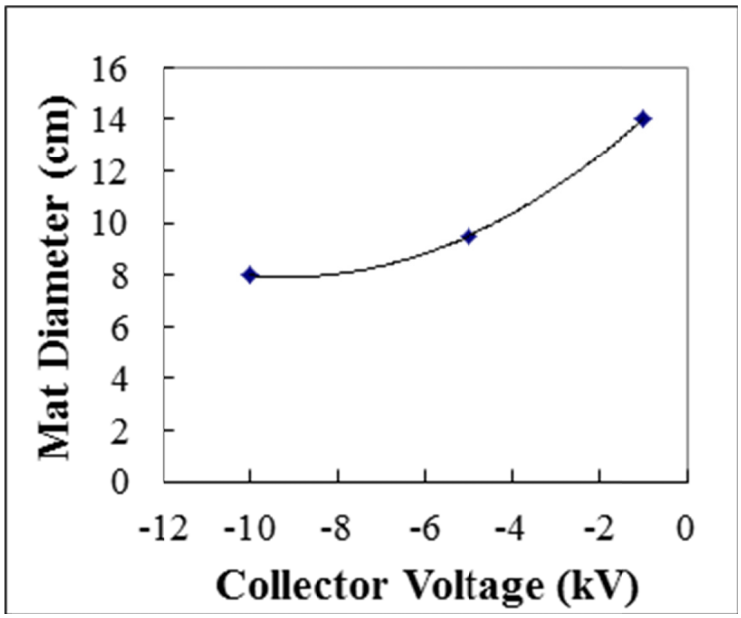

Figure 7: *Plot of the mat size and collector voltage relationship for a 10% w/v Pellethane solution in 70:30 THF:DMF at 35 cm distance between the 20 gauge needle at +15 kV and the collector and a flow rate of 75 µL/min.*

3.1.2 Effect of solvents

The solvent used for electrospinning serves several roles: it solvates the polymer, affects the surface tension, and determines how quickly the fibre dries. Some of the intrinsic solvent properties of tetrahydrofuran and N,N'-dimethyl formamide, which were used to dissolve the Pellethane, are presented in Table 1. THF has higher vapour pressure than does DMF, indicating that electrospun fibres containing more THF will dry faster than fibres with more DMF. The viscosity and surface tension of THF are both lower than for DMF. Both solvents readily dissolved Pellethane and different ratios of THF:DMF were tested to determine optimum electrospinning conditions. Ratios tested included 100:0, 90:10, 70:30, 60:40, and 50:50 THF:DMF containing 10% w/v Pellethane.

Table 1: *Properties of THF and DMF solvents.*[25]

Property (20°C)	THF	DMF
Vapour Pressure (Torr)	143	2.7
Viscosity (cP)	0.55	0.92
Surface Tension (mN/m)	26.4	36.76
Density (g/cm)	0.888	0.9487

As expected, fibre mats electrospun from the 10% w/v Pellethane in 100% THF solution showed a low degree of fusing, due to the high vapor pressure of the solvent, which resulted in dry fibres arriving at the collector. This solution, however, dried so quickly that the needle clogged after a short period of electrospinning. Needle clogging was also accompanied by the formation of a very tight electrospinning envelope through which the fibres travelled, and only covered a small portion of the collector, even for large needle-collector separations and high voltages on the needle (15 kV). Instabilities during fibre flight caused the fibre trajectory to cover a larger area over time. Fibres produced from this solution contained a high portion of beads similar to solutions with lower Pellethane concentrations, though these beads had dimpled surfaces, Figure 8. Rapid solvent evaporation in humid environments has previously been observed to result in the formation of pores within the fibre structure due to the condensation of water droplets on the surface which is cooled by the solvent evaporation.[18]

Fibres electrospun from 90:10 THF:DMF solutions showed a marked decrease in the number of beads and fewer dimples were observed, Figure 8. The needle was still prone to clogging though the spinning envelope was larger. Images of fibre mats electrospun from solutions with higher DMF content are also shown in Figure 8, and were achieved over a range of experimental conditions, Table 2. A consequence of increased DMF concentration was the collection of wet fibres that fused together. Fibre fusing was minimized by increasing the needle-collector distance and reducing the solution flow rate. The voltage difference between the needle and collector, used to drive the electrospinning, was in the range of 650 to about 700 V/cm.

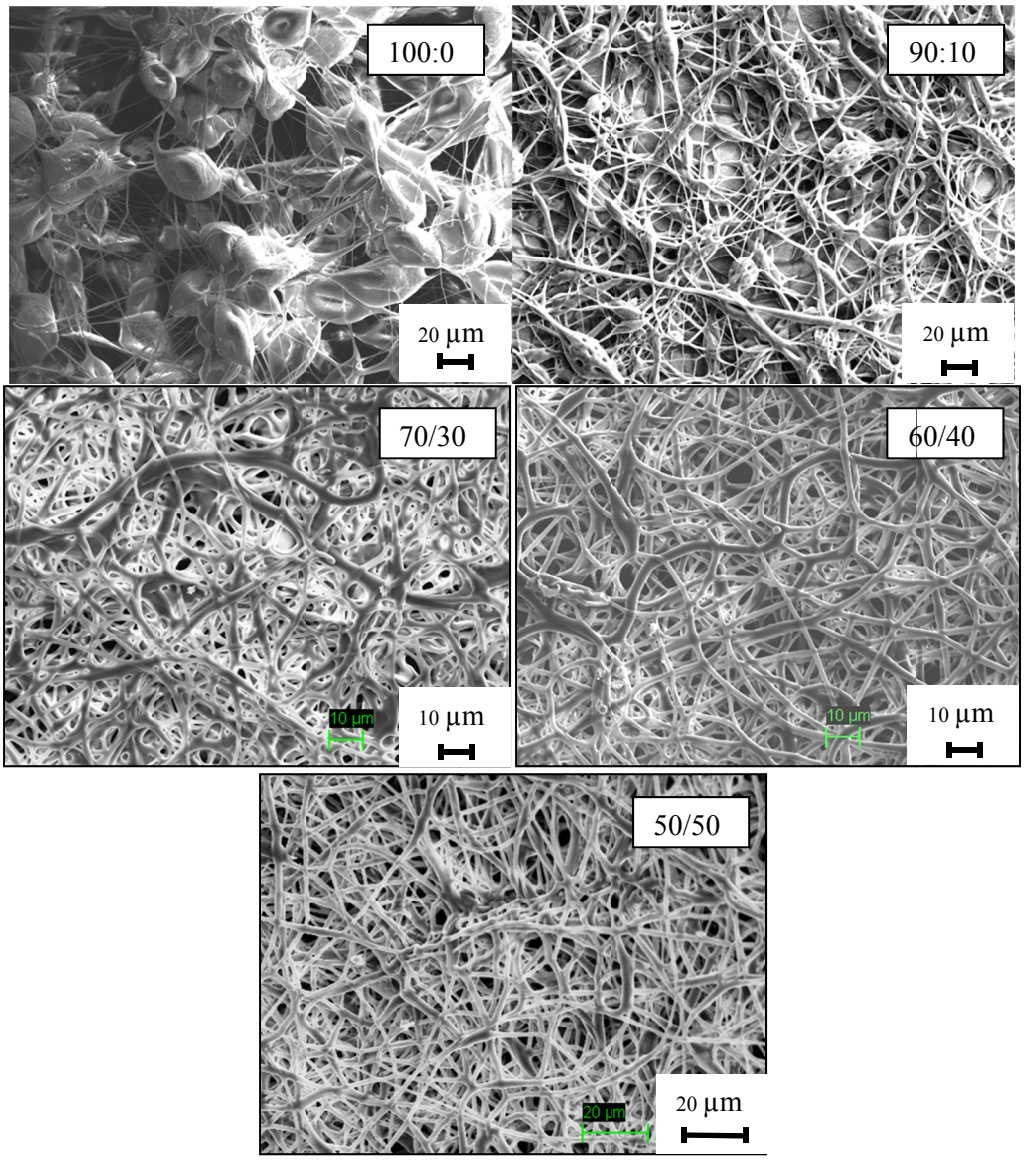

Figure 8: *SEM images of electrospun 10% w/v Pellethane in THF:DMF ratios as indicated on the images. Electrospinning parameters presented in Table 2.*

Table 2: *Electrospinning parameters for fibres electrospun from 10% w/v Pellethane in THF:DMF solutions as presented in Figure 8.*

THF:DMF ratio	Flow rate (µL/min)	Needle Gauge	Needle-Collector Distance (cm)	Needle Voltage (kV)	Collector Voltage (kV)
100:0	50	30	30	15	-5
90:10	50	20	35	15	-10
70:30	25	20	35	-10	13
60:40	25	20	35	-10	13
50:50	25	20	35	-10	13

3.1.3 Effect of polymer viscosity

In addition to the solvent evaporation rate, the electrospinning process was affected by the solution viscosity. The viscosities of 70:30 THF:DMF Pellethane solutions with concentrations of 5, 7.5, 10 and 15 w/v % were measured, Figure 9. The viscosity of other solvent ratio Pellethane solutions were also measured and were observed to have only a minor effect on the viscosity, as did the addition of 1 w/v % titanium dioxide nanoparticles. The major factor determining the solution viscosity is the polymer concentration which is expected to increase as polymer chain entanglements increase. Measurements made at room temperature, about 23 ± 1°C, are summarized in Table 3.

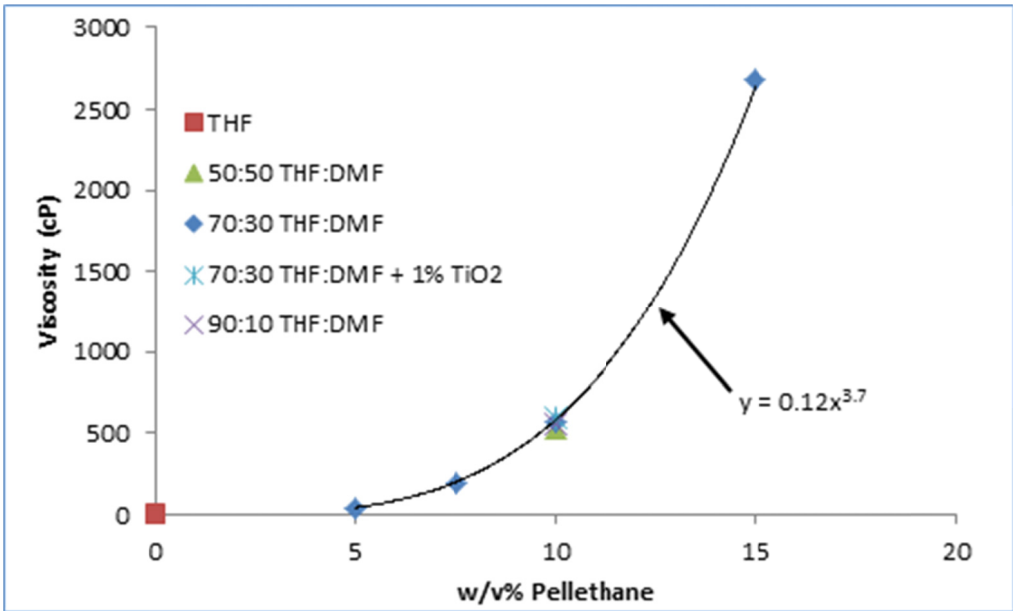

Figure 9: *Plot of measured solution viscosities as a function of Pellethane w/v %, at room temperature. The plot also shows several THF:DMF ratios at 10% w/v polymer. The points are the average of three measurements.*

Table 3: *Viscosities of Pellethane in 70:30 THF:DMF as a function of the polymer concentration.*

Solution	Concentration (% w/v)	Viscosity (cP)
DMF	0	0.92
THF	0	0.55
70:30 THF:DMF	5 7.5 10 15	45 195 576 2690
70:30 THF:DMF +1% TiO_2	10	590
50:50 THF:DMF	10	526
90:10 THF:DMF	10	558

The increase in the solution viscosity noticeably affected the electrospinning characteristics, such as the size of the Taylor cone, the rectilinear region length, the size of the electrospinning envelope, as well as the morphology of the electrospun fibres. As the polymer concentration increased, the rectilinear length increased, there was less whipping, and the spinning envelope became narrower with a commensurate decrease in the mat size. Note that fibre stretching is said to occur in the spinning envelope, so a reduction in the size of the spinning envelope should equate to thicker fibres. This is observed in the SEM images of electrospun fibres as the polymer concentration increased, Figure 10. Low polymer concentrations resulted in fine fibres containing beads. Under the strobe light, the envelope cone for the 5% w/v Pellethane solution appeared to contain secondary whipping that was not observed for higher polymer concentrations. At high polymer concentrations no beads were observed and the fibre diameters were larger. Note, a larger needle diameter and higher applied potential were required to electrospin the 15% w/v polymer solution. The fibres formed from this solution were mostly above 2 μm in diameter and minimal fusing was observed under some experimental conditions. The 20% w/v polymer solution was electrospun using the 15 gauge needle under the force of gravity. The drop was formed on the end of the needle with the assistance of the plunger to allow electrospinning to begin. This solution resulted in thick fibres and no whipping motion was noticed. The fibres collected in tight bundles on the mat and were large enough to be seen by eye.

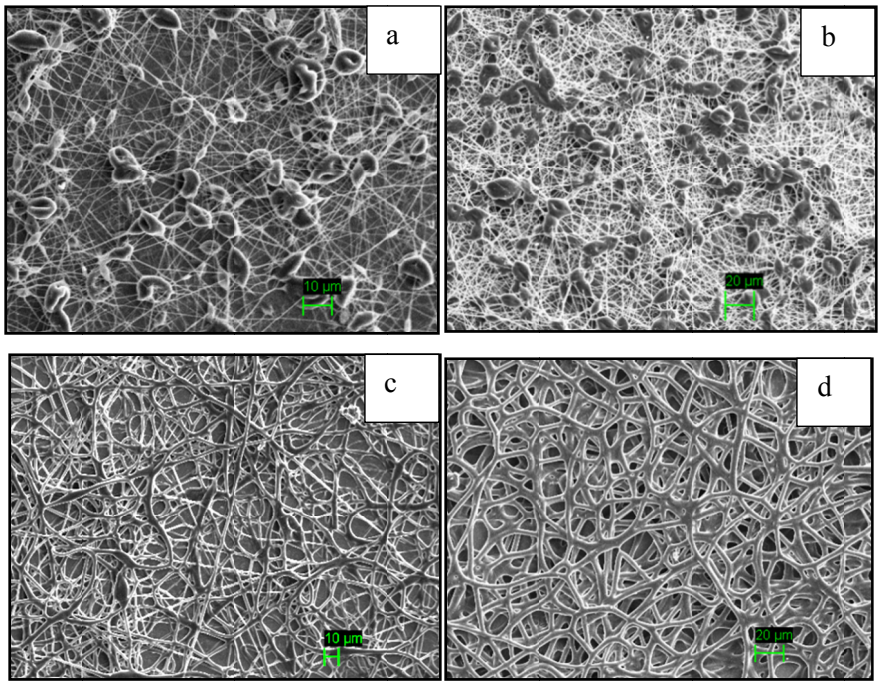

Figure 10: *SEM images fibres produced from (a) 5%, (b) 7.5%, (c) 10% and (d) 15% Pellethane solutions under identical experimental conditions of a 35 cm distance, 20 gauge needle, +15 kV at needle, -10 kV at the collector and an injection rate of 75 µL/min.*

The diameters of fibres were measured for each mat. The maximum and minimum diameters are plotted in Figure 11 as a function of the polymer concentration, and needle-collector distance. In each case the diameter increased with polymer concentration for both the maximum and minimum sizes. It was also noted that the range of diameters increased with the solution viscosity or polymer concentration. The lower right hand plot in Figure 11, presents the average jet length as a function of polymer concentration which was found to increase, indicating an increase in jet stability with concentration.

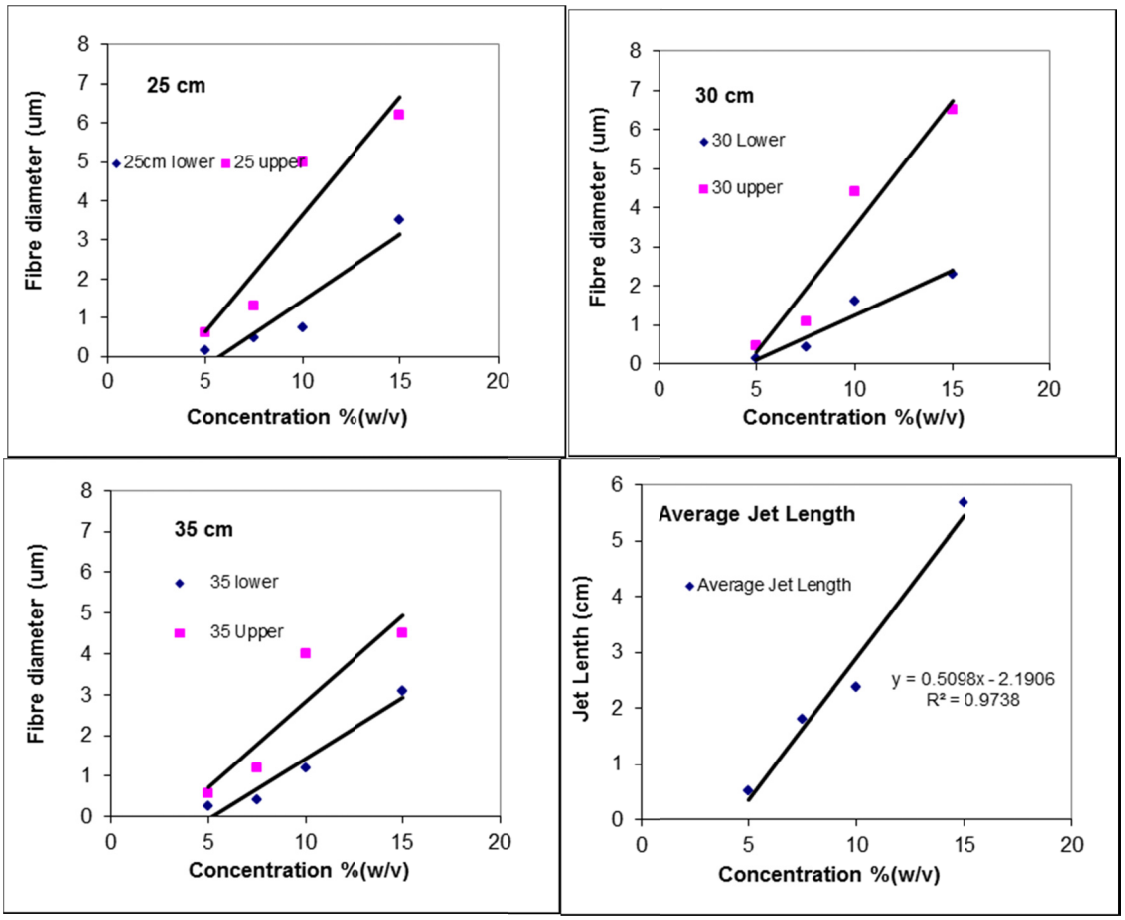

Figure 11: *Fibre diameter as a function of polymer concentration and needle-collector distance. Pink points indicate the upper limit of fibre diameters measured, and blue points indicate the lower limit. Also plotted is the average jet length as a function of polymer concentration. Experimental conditions of 20 gauge needle, +15 kV at the needle, -10 kV at the collector, and 75 µL/min injection rate were constant.*

3.1.4 Effect of polymer solution flow rate

The flow rate of the polymer solution through the needle was found to have an effect on the fibres in the electrospun mats, including the fibre diameter and fibre fusing which occurred when wet fibres were collected. For the vertical gravity feed orientation, the flow rate was originally controlled through the use of different gauge needles with the optimum size being dependent on the solution viscosity and amount of solution in the syringe. The more concentrated solutions required smaller gauge needles, or larger openings, to allow the more viscous solutions to drip out of the syringe, and larger gauge needles were required to limit the flow of less viscous solutions. In the horizontal orientation with a syringe pump, the needle gauge was less important to the electrospinning process because the flow rate was controlled by the pump. The optimum needle choice for this orientation, and each of the solutions prepared, was determined by evaluating the electrospun fibres for wetness, beading, spinning stability, and other factors such as dripping and

ability to even electrospun a fibre. The results are summarized in Table 4. The term "Worked" indicates that the conditions produced acceptable fibres, while the term "Best" indicates that the fibres were superior, i.e. not fused, uniform, etc.

Table 4: *Optimum needle gauge as a function of polymer concentration.*

Needle Gauge/ Concentration	5%	7.5%	10%	15%
24	Best	Worked	Worked	Too Viscous
20	Worked	Worked	Best	Worked
15	Dripped	Not Used	Worked	Best

The flow rate of the solution through the needle had an impact on the fibre characteristics, with larger diameter fibres being obtained when the flow rate was high. High solution flow rates also resulted in an increase in the amount of fusing in the mats due to the formation of thicker wetter fibres, or the coalescence of wet beads which formed from lower concentration solutions, Figure 12a. Decreasing the flow rate reduced the amount of fused material which resolved into beads Figure 12b-e. Thus it is assumed that under these conditions, beads are arriving at the collector still very wet. The amount of fusing was qualitatively evaluated on a scale of 0–10 with zero being unfused and 10 being completely fused fibres. Fusing was identified where adjacent fibres, or beaded regions, were joined with no distinct boundaries. The fusing quality is plotted for electrospun 10% w/v Pellethane solutions, at flow rates of 25, 50, and 75 µL/min for THF:DMF ratios of 100:0, 90:10, 70:30, 60:40, and 50:50, from a 20 gauge needle at +15 kV positioned 35 cm from the collector plate at -10 kV, Figure 13. Electrospinning was continued for five minutes and the fibre mats were subsequently examined under the SEM. The expected trend was for the degree of fusing to increase with the percentage of DMF, and as the flow rate increased. The average degree of fusing increased from 2.5 to 4.8 to 7 as the flow rate was increased from 25 to 75 µL/min and is highly correlated. The effect of DMF on fusing was not as clear. The amount of fusing was generally lower for the 100:0 and 90:0 than for the 70:30 and 60:40 THF:DMF solutions. However, the degree of fusing for the fibres prepared from 50:50 THF:DMF appear to be anomalous. The lower right plot in Figure 13 considers the effect of a smaller needle-collector distance of 25 cm. It is observed that the degree of fusing was larger for the shorter needle-collector distance which is consistent with the shorter flight path and less time for the solvent to evaporate before the fibres or beads contacted each other.

It was observed that production of stable electrospinning conditions required a commensurate increase in the applied potential for flow rates up to 100 µL/min. At flow rates higher than 100 µL/min there was not as great of a change in the upper and low fibre diameter limits. The flow rate also affected the length of the rectilinear region. The length of the jet was proportional to the flow rate and the formation of thicker fibres.

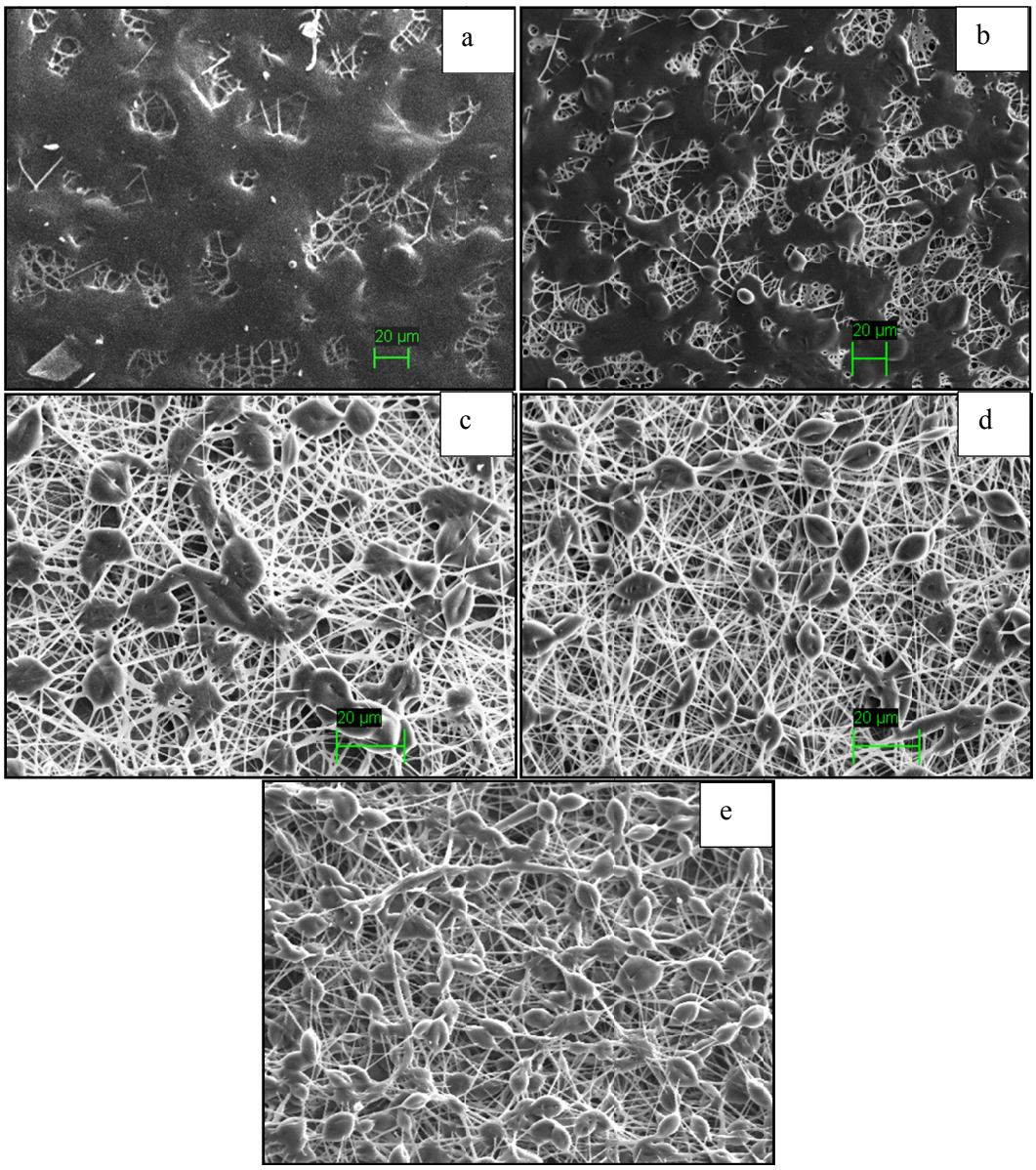

Figure 12: *SEM images of the fibre mats produced as a function of flow rate: (a) 125 µL/min, (b) 100 µL/min, (c) 75 µL/min, (d) 50 µL/min and (e) 25 µL/min, using a 7.5% Pellethane solution in 70/30 THF:DMF, 20 gauge needle, -10 kV collecting voltage, and a distance of 35 cm.*

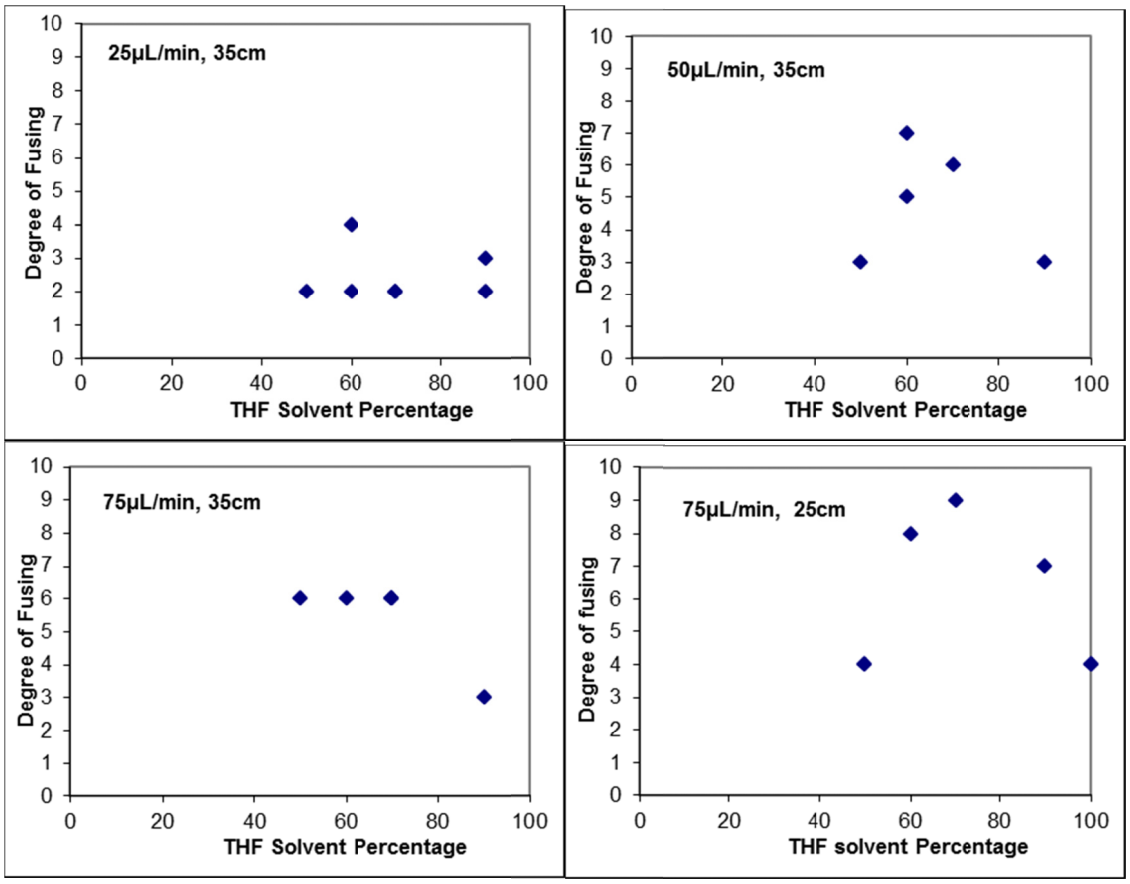

Figure 13: *Degree of fusing for10% Pellethane solutions as a function of solvent composition and pump rate. Experimental conditions were: Needle gauge of 20, Needle voltage +15 kV, Collector Voltage -10 kV.*

3.1.5 Effect of nanoparticles

In order to increase the surface roughness, titanium dioxide nanoparticles were added to Pellethane solutions at loadings of 1 and 5% w/v, to 5, 10 and 15% Pellethane solutions. The effective dispersion of the titanium dioxide nanoparticles was found to depend on the polymer concentration. At low polymer and high titanium dioxide loadings, residual nanoparticles were found at the bottom of the solution, whereas solutions containing 5% titanium dioxide in 15% polymer were completely dispersed.

Electrospun fibres from 5% w/v Pellethane solutions containing either 1% w/v, or 5% w/v titanium dioxide, exhibited many beads and very fine fibres, similar to the electrospun material containing only 5% polymer, Figure 14. The fibres, in the material electrospun from solutions containing 5% titanium dioxide and 5% polymer, were just visible under the SEM.

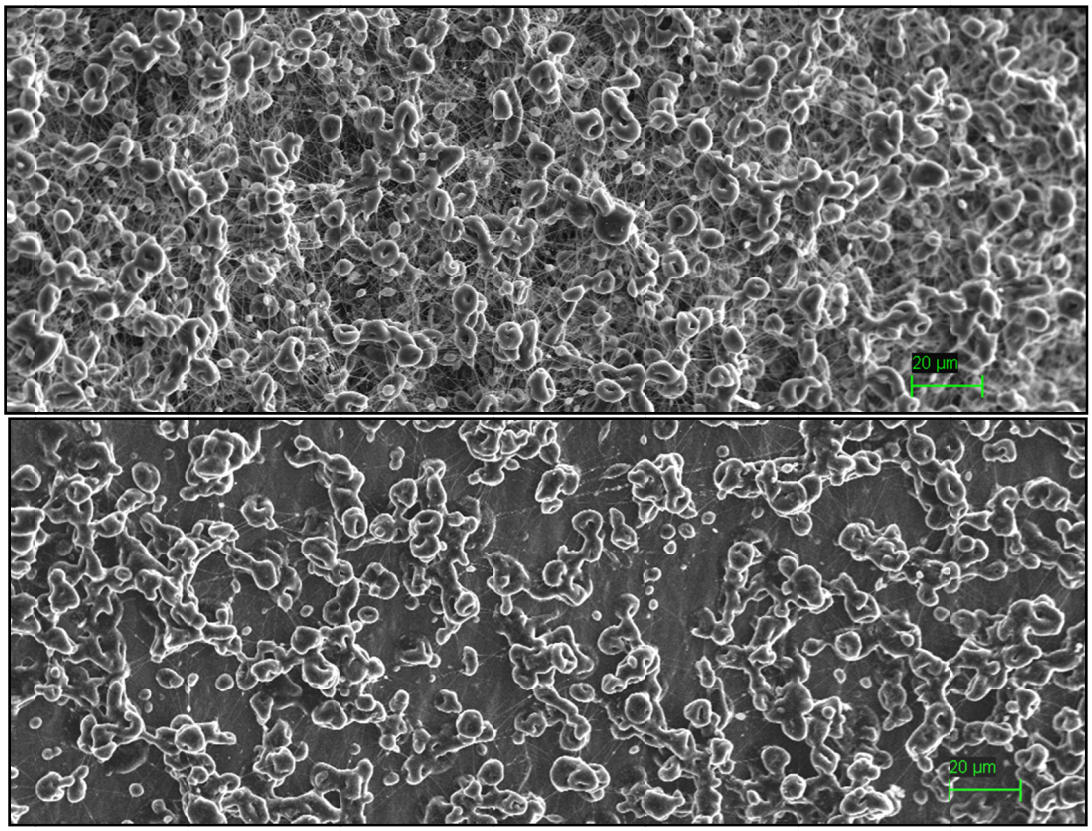

Figure 14: *SEM images of 5% w/v Pellethane solutions containing 1% w/v (top) and 5% w/v (bottom) titanium dioxide. Both solutions were electrospun at a needle to collector distance of 35 cm from a 20 gauge needle with a flow rate of 25 µL/min.*

Fibres electrospun from 10% w/v polymer solutions containing nanoparticles, Figure 15, were found to contain beads, contrary to the findings for 10% pure polymer which did not, Figure 10c. The beads were found to fuse for both 1% and 5% w/v nanoparticle solutions and different solution flow rates. The use of a smaller needle, 24 gauge, significantly reduced bead formation and fusing when electrospun at polymer solution flow rates of 25 or 50 µL/min, Figure 16. Note that magnifications of the images in Figures 15 and 16 are not identical.

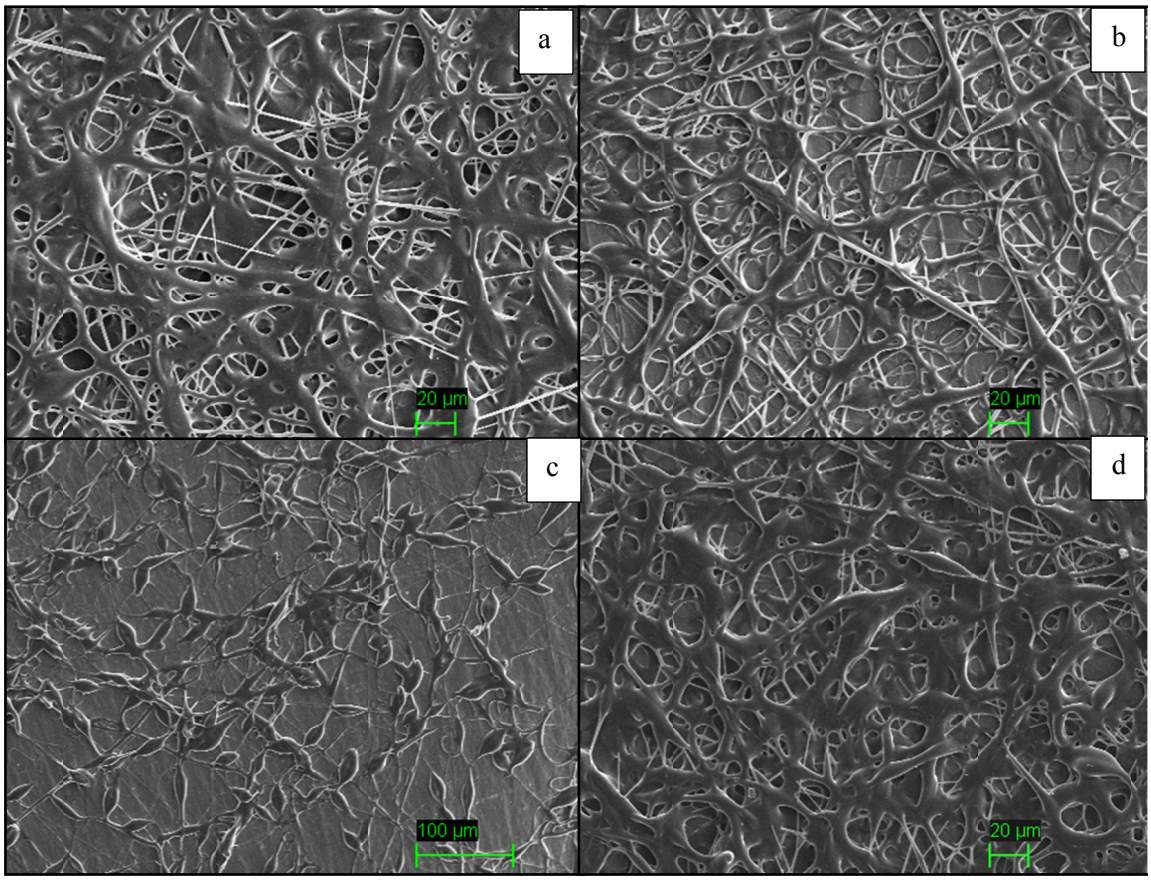

Figure 15: *SEM images of fibres electrospun from 10% w/v Pellethane solutions containing 1% w/v TiO_2 with a 20 gauge needle at the flow rates of (a) 100 µL/min, (b) 75 µL/min, (c) 50 µL/min, and (d) 25 µL/min.*

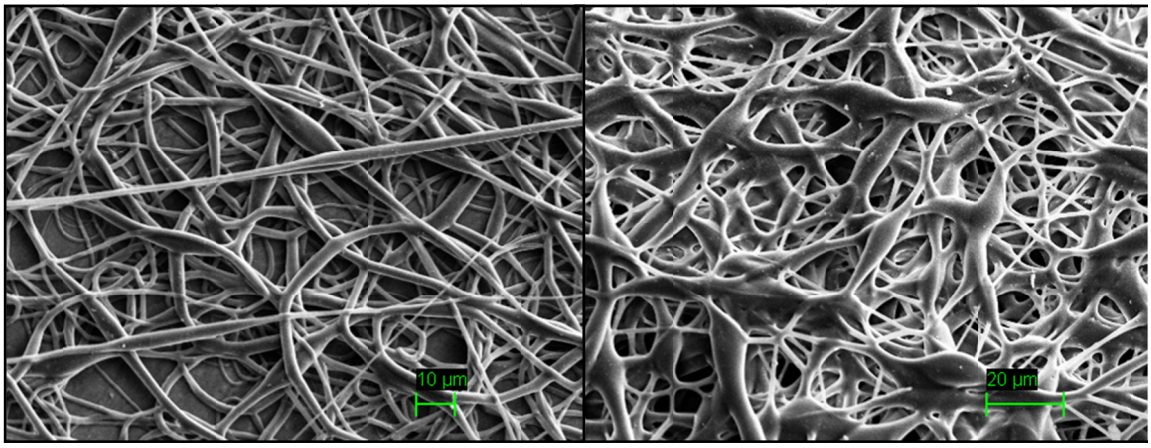

Figure 16: *SEM images of fibres electrospun from (left) 10% w/v Pellethane solutions containing 1% w/v TiO_2 with a 24 gauge needle at flow rates of 50 µL/min (left), and 25 µL/min (right).*

Bead formation was similar for fibres electrospun from 10% w/v Pellethane solutions containing 5% w/v titanium dioxide, and a bead free fibre mat was obtained for a flow rate of 10 µL/min, Figure 17. Flow rates other than 10 µL/min showed a significant amount of fusing between fibres.

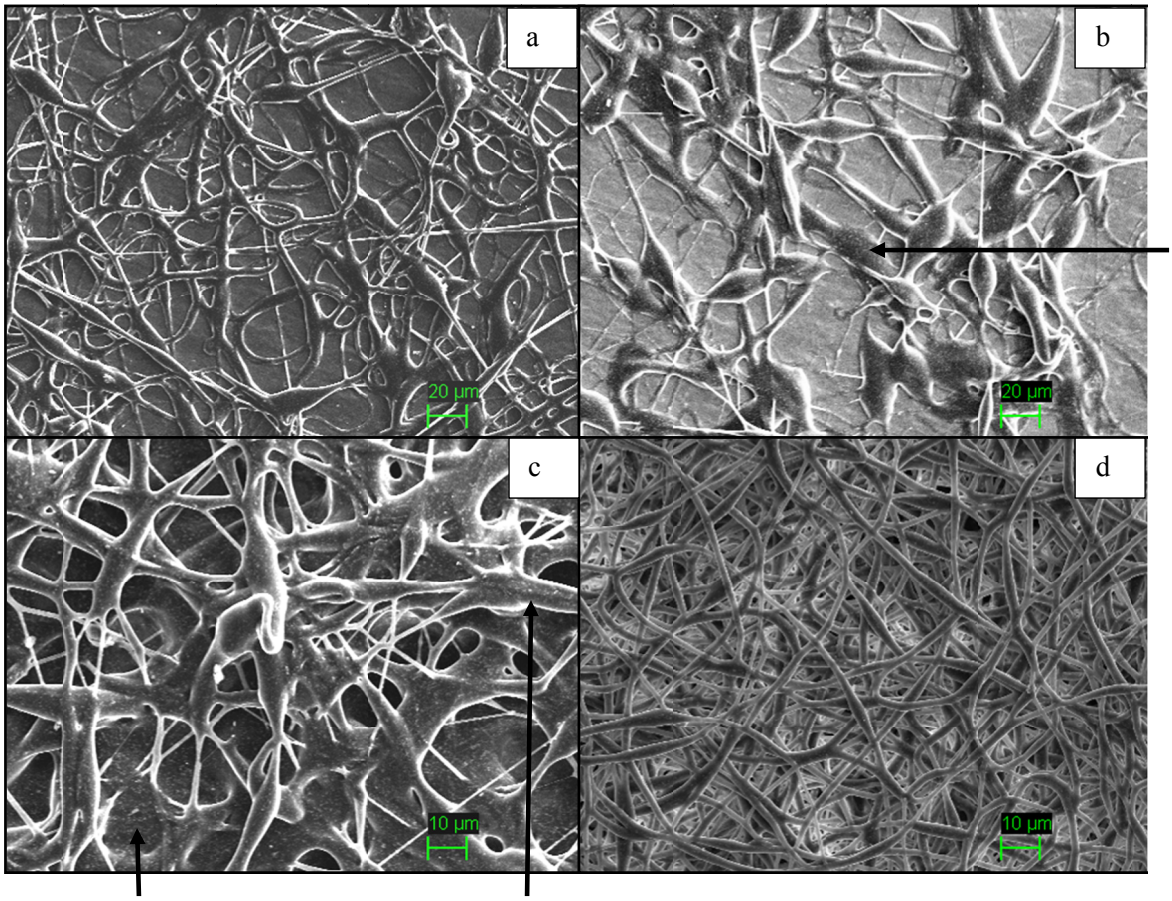

Figure 17: *SEM images of fibres electrospun from a 10% w/v Pellethane solution containing 5% w/v TiO_2 with a 20 gauge needle at flow rates of (a) 75 µL/min, (b) 50 µL/min, (c) 25 µL/min, and (d) 10 µL/min. Light grainy spots on the fibres are attributed to the titanium dioxide, arrows.*

Fibre mats electrospun from 15% Pellethane solution loaded with 5% TiO_2 were similar to fibres electrospun from 15% Pellethane solutions containing no nanoparticles.

All materials electrospun from solutions containing nanoparticles were visibly rougher under the SEM than fibres electrospun from neat polymer solutions, Figure 10c. Nanoparticles were visible on the surface or in the fibres and beads. The titanium dioxide particles with a diameter of about 100 nm resulted in the fibres having micron and submicron scale roughness.

Previous studies of mixtures of polyethylene oxide and titanium dioxide have shown an increase in solution viscosity with the addition of the nanoparticles, permitting the electrospinning of more dilute polymer solutions.[21] This observation indicates that fewer beads should be formed due to the increase in viscosity, however, the opposite was observed for electrospun polyurethane-titanium dioxide fibres. The viscosity measurements of the Pellethane-titanium

dioxide solutions were not significantly different from the neat polymer solution. This may indicate less polymer-nanoparticle interaction than was observed for polyethylene oxide.

3.2 Hydrophobicity

In order to determine the effect of fibre properties on the hydrophobicity, 5 µL water drops were placed on the surface of the fibre mats, and contact and tilt angles were measured using a Keyence Digital microscope and a tilting stage, respectively, Figure 18.

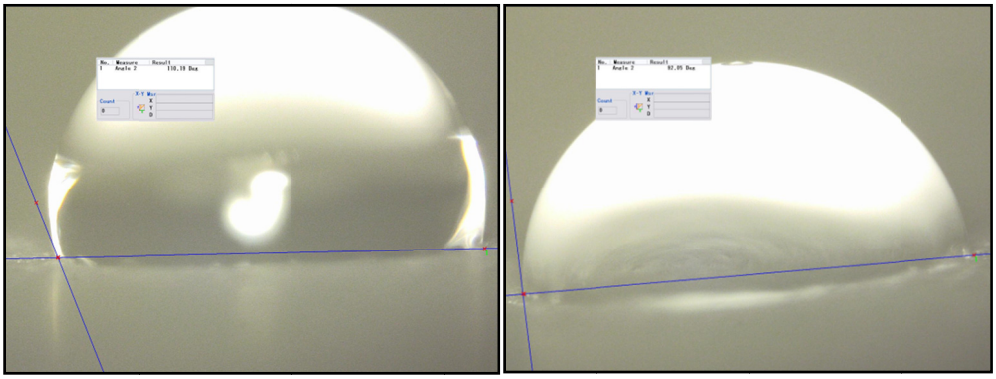

Figure 18: *Water contact angle measurements for a Pellethane fibre mat electrospun from a 15% w/v solution, with a flow rate of 50 µL/min, through a 15 gauge needle at +15 kV and 35 cm from the collector -5 kV. The original state showing a contact angle of 110° (left) and the same water droplet after a shock produced a contact angle of 92° (right). These images were recorded as the tilt angle was being measured, which is why the substrate appears to be tilted.*

As a reference, Pellethane was spin coated from a 5% solution onto a glass slide in order to produce a smooth film and determine the contact angle due to only the material's chemical properties. The average contact angle of the smooth spin coated Pellethane sample was 73° which, being less than 90°, indicates that the surface is hydrophilic. Water drops placed on the smooth Pellethane surface did not roll off when the substrate was tilted, indicating high solid-liquid surface tension between the water and the Pellethane, likely due to hydrogen bonding between the urethane linkages from the polymer and the water molecules.

Contact angles measured for electrospun Pellethane fibre mats ranged from 110–126° and were larger than the contact angles measured for the spin coated Pellethane surface. Higher contact angles were measured for fibre mats with few beads, little fusing, and for those mats that were built up into thick layers. Thin mats, where there was not a sufficient number of fibres to support the water drop above the aluminum foil, resulted in contact angles of 62°, lower than measured for the spin-coated Pellethane. A measure of the areal density of the fibre mats and their thickness would be useful for comparing different samples, however, this was not undertaken. The contact angle increased as the degree of fibre fusing decreased. This is expected as a highly fused surface should approximate the spin coated state. The increase in contact angle from 73° for a smooth surface to 110–126° for the rough fibre mat could be indicative of either the Cassie-Baxter or Wenzel states. The metastable nature of the Cassie-Baxter state was observed for the drop shown in Figure 18, when a shock to the sample resulted in the drop changing shape, and the contact angle decreased from 110° to 92°, as the system transitioned from the Cassie-Baxter state to the Wenzel state.

Tilt angles could not be measured for the electrospun Pellethane fibre mats as the water drops remained adhered to the surface at all tilt angles. In part this is due to the hydrophilic nature of the polyurethane polymer, however, it was also observed that pinning of the drop to the surface occurred if fibres were wetted and embedded in the drop and some drops may have been in the Wenzel state.

A spin coated 5% w/v Pellethane solution containing titanium dioxide particles resulted in an average contact angle of 81°, higher than the spin coated polymer alone. This increase in contact angle was also noted for most of the electrospun nanoparticle containing fibre mats where the measured contact angles ranged from 114–142°. The higher contact angles obtained are most likely a result of the secondary roughness provided by the nanoparticles. Pinning of the water drops was still evident for these materials, even though in some cases the contact angles were considerably higher. This indicates that the surface tension and other pinning mechanisms are still too large to permit the water to release from the surface. Reduction of the solid-liquid surface tension could be achieved by the addition of polymers with a greater hydrocarbon or fluorocarbon component and fewer hydrophilic groups. The use of hydrophobic derivatized nanoparticles could also reduce the solid-liquid surface tension.

The literature reports that contact angles were larger for beaded electrospun fibre mats and attributed this observation to the presence of a second level of roughness.[20] The impact of beads on the fibres on the contact angle will depend on the size of the beads and fibres; the ability of the distribution of sizes to support the water drop; and the effective contact area. Large beads may increase the contact area, reducing the contact angle, while small beads may have the opposite effect.

3.2.1 Sol-gel coating

A sol-gel coating technique was used to derivatize the surface of electrospun fibre mats, several textiles, and other materials. The sol-gel coating, used to reduce the solid-liquid surface tension and to produce a nanoscale roughness, was applied by dipping the materials into an activated mixture of alkoxy silane, TEOS, and FAS. The components were in a 10:1 ratio of TEOS to FAS (mol:mol). As this mixture reacts, a silicate core grows that is size limited by a corona of fluorinated silicate groups. This process produced a nanoscale rough hydrophobic coating on the substrate. Spin coated Pellethane on a glass slide, Polyester, cotton, and glass fibre textiles, and electrospun fibre mats were dipped into the sol-gel mixture, dried, and their water and oil contact and tilt angles were measured, and these results are summarized in Table 5. SEM images of the fibre surfaces and pictures of the water drops on the surface before and after sol-gel coating are presented in Figures 19–24 and Figures A.1 to A.7 in the annex. The water contact angle was found to increase for each material after it was sol-gel coated, with the contact angles falling in the range of 140 to greater than 150°. Tilt angle measurements were also made of these materials, and range from greater than 47° to less than 5°. Drops of vegetable oil placed on the coated surfaces tended to wet the material and seep into it.

Table 5: *Sol-gel coating preparation and characteristic summary.*

Substrate	Water Contact and Tilt Angles*			Comments on Substrate Preparation and Coating
	Before Coating	After sol-gel Coating	Avg. Tilt Angle	
Spin coated Pellethane on Glass Slide	72.9	141.8	18.5	5% w/v Pelletane in a 70:30 THF:DMF solution was used for spin coating.
Textile: PET-thick	--	148.9	24.6	Substrates washed with ethanol then dipped into the sol-gel suspension before air drying
Textile: PET thin	51.1	146.4	31.6	
Textile: Cotton	145.5	149.8	21.6	
Textile: Glass fibre	118.7	142.7	19	
Electrospun: E344	124.4	140.4	>47	Electrospun fibre samples. A sample taken for the original specimen was coated in the same manner as the fabric substrates.
Electrospun: E371	122.8	144.9	>47	
Electrospun: E384	119.2	153.6	<5	
Electrospun: Removed Thick	114.6	146.9	4.5	This thick sample was removed from the collector foil and coated

* Contact angle measurements using peanut oil were attempted for each of the coated and native substrates, however, it was found that the peanut oil seeped into each surface and contact angle measurements were not possible. An exception was for the sol-gel coating on the Pellethane spin coated glass slide. Contact angle was not recorded. A tilt angle was measured for this sample of 40° and the oil slowly slid down the surface, leaving a trail behind.

The sol-gel coating on Pellethane spin coated onto a glass slide, resulted in an increase in the contact angle from 73° to 142°. The tilt angle measured for this surface was 18°. As a baseline this indicates that the sol-gel is responsible for a large increase in the contact angle of a nominally smooth surface.

A thin plain weave PET textile before being coated with the sol-gel is shown in Figure 19. The inset pictures show a water drop just after being placed on the textile and after several seconds. During this time the water drop has wet the textile and spread out. The contact angle measured just after deposition was about 51°. After sol-gel coating, the fibres appear to have a glassy coating which at higher magnification, inset, appears as a rough surface, Figure 20. Water drops placed on the treated textile beaded to high contact angles around 146°. The tilt angle at which the drop started to slide across the surface was measured to be about 32°, which indicates that adhesion between the water and surface is still relatively strong. Images of other textiles, pre- and post- sol-gel treatment, and water drops on the surface are presented in the annex, Figures A.1 to A.7. In each case the surface of the treated fibres appeared rougher and the contact angle increased. The tilt angle for the sol-gel coated textiles ranged from between 20–30°.

In the same manner electrospun polyurethane fibre mats were sol-gel coated. SEM images of the fibre mats reveal that a rough coating deposited on the fibres during this process, Figures 21–24. The electrospun fibre mat presented in Figures 21 and 22, was relatively thick with little fusing or beading. The contact angle increased from 124° to 140° on coating, though the drops were still pinned to the surface at the limit of the device of 47°.

A beaded electrospun fibre mat was also sol-gel coated and these images are presented in Figures 23 and 24. The sol-gel coating on these fibres appeared to be heavier than was observed for the mat in Figure 22, with the coating forming a very rough surface. The contact angle exceeded 150° and a tilt angle of less than 5° was measured, qualifying this as superhydrophobic.

In an attempt to see if the supporting substrate (the aluminum foil used to coat the collector) had an effect on the sol-gel deposition process and contact angle measurements, a thick electrospun mat was selected and removed from the aluminum foil. The contact angle of the untreated material was measured to be about 115°. On sol-gel coating, the contact angle increased to about 147° and a tilt angle of 4.5° was measured. These results which are similar to those of sample E384, indicate that the substrate is probably not affecting the contact angle when the fibre mat is thick. Images of this material are not presented.

An important finding for the materials studied here was that the sol-gel treatment increased the contact angles, for water on the substrates, to values near 150°. A second important finding was that although the contact angle was high, the drops often remained pinned to the surface even at very high tilt angles. A major feature of superhydrophobic materials is that the liquid should roll away when the surface is tilted. This will reduce surface wetting and can act as a cleaning mechanism, where the rolling liquids carry away dirt particles of the surface. Pinning of the liquid to the surface may have occurred while placing the liquid onto the surface. It was difficult to get the water onto the sol-gel coated surface as the adhesion of water to the coating was lower than the adhesion of the water to the syringe used to deposit the liquid. It may be that while trying to get the liquid onto the surface the liquid was forced into the fibres, resulting in the Wenzel state, or as has been observed, to have caused the liquid to be wrapped around fibres in the surface. Finally, the combination of the surface roughness, from the electrospun fibres and the sol-gel coating, appears to be necessary in order to achieve high contact angles and low tilt angles. More work is required in order to produce definitive results.

The results presented here, provide guidance for electrospinning fibrous mats. Electrospun fibres have high surface areas. The ability to include fillers, functional groups, control the polymer chemistry, and coat the fibres means that they are of interest as catalysts, filtration membranes, and as functional textiles. Methods for increasing the roughness and reducing the surface energy of the materials have also been presented, and superhydrophobic materials were demonstrated. Superhydrophobic materials may find applications in rainwear, self-cleaning, corrosion reduction, and personnel and equipment protection from chemical agents. The fibrous materials studied here may be useful for applications involving textiles, or in filtration systems such as oil/water separation. Material durability needs to be considered, as does other methods for producing rough low surface energy coatings. Commercially available superhydrophobic products with high durability are sparse.

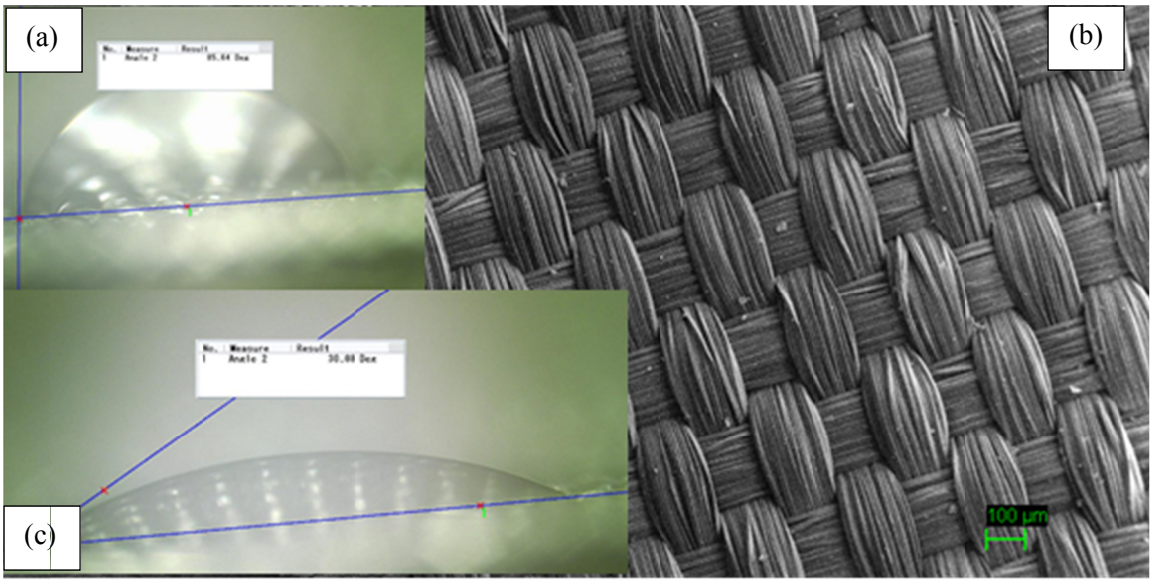

Figure 19: *SEM and microscope images of thin PET textile prior to sol-gel coating.*
(a) Image of a 5 µL water drop immediately after placement,
(b) fabric structure, and (c) water drop a few seconds after placement.

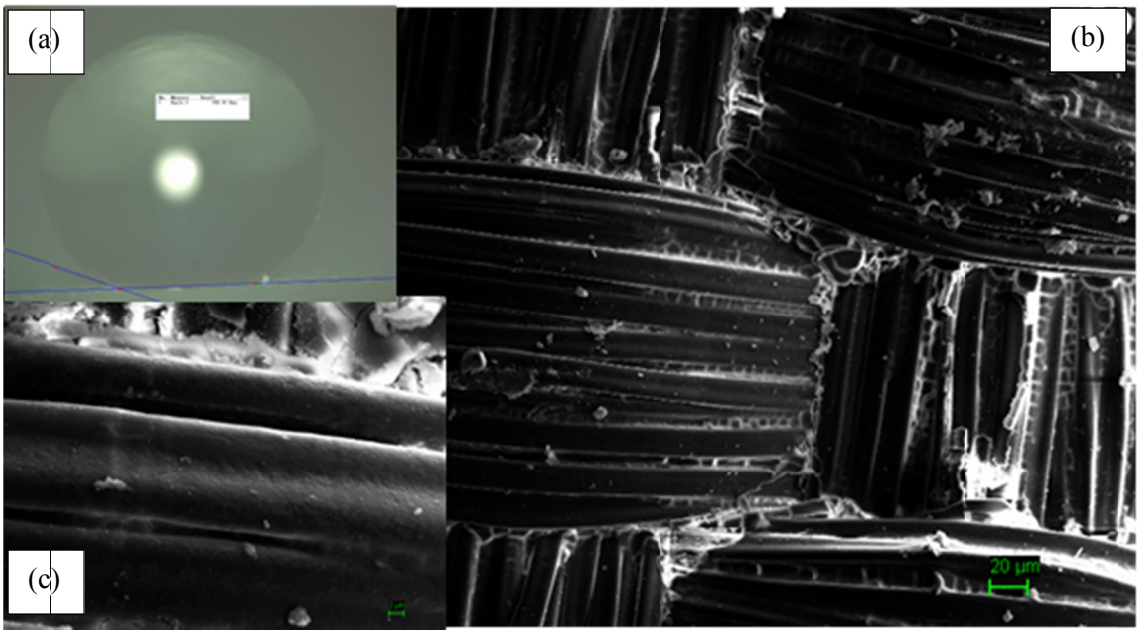

Figure 20: *Images of a thin PET textile after sol-gel coating.*
(a) Image of a 5 µL water drop on the coated textile,
(b) SEM image of the coated textile structure,
and (c) enlarged PET strand showing the added texture from the sol-gel coating.

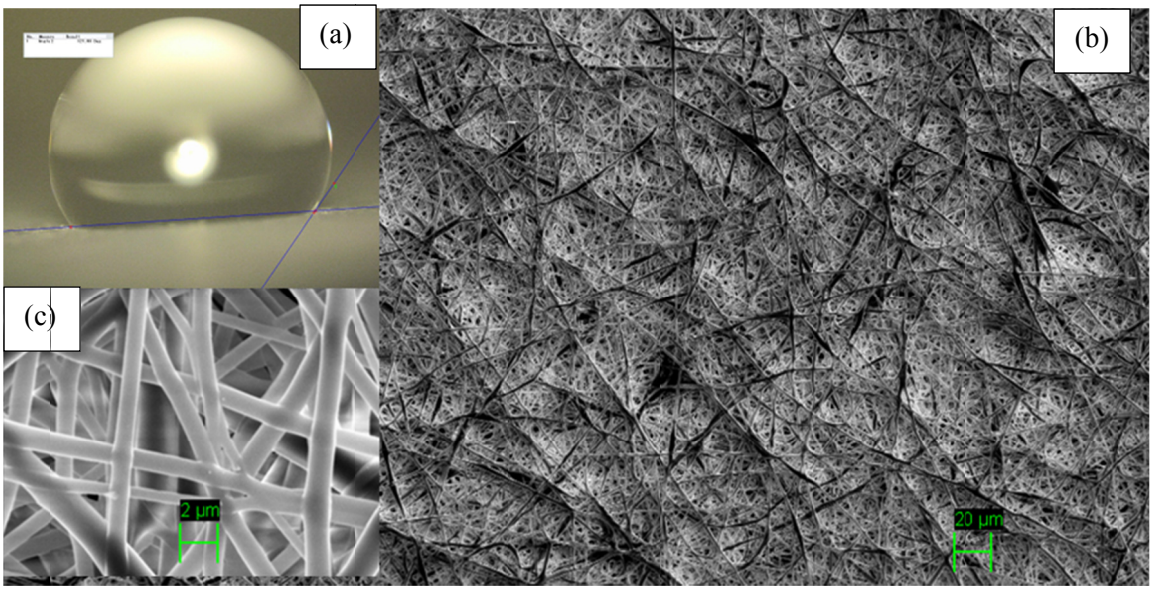

Figure 21: *SEM and digital microscope images of uncoated E 344.*
(a) Water contact angle measurement, (b) SEM image of electrospun fibre mat,
(c) enlarged SEM image showing the fibres' texture.

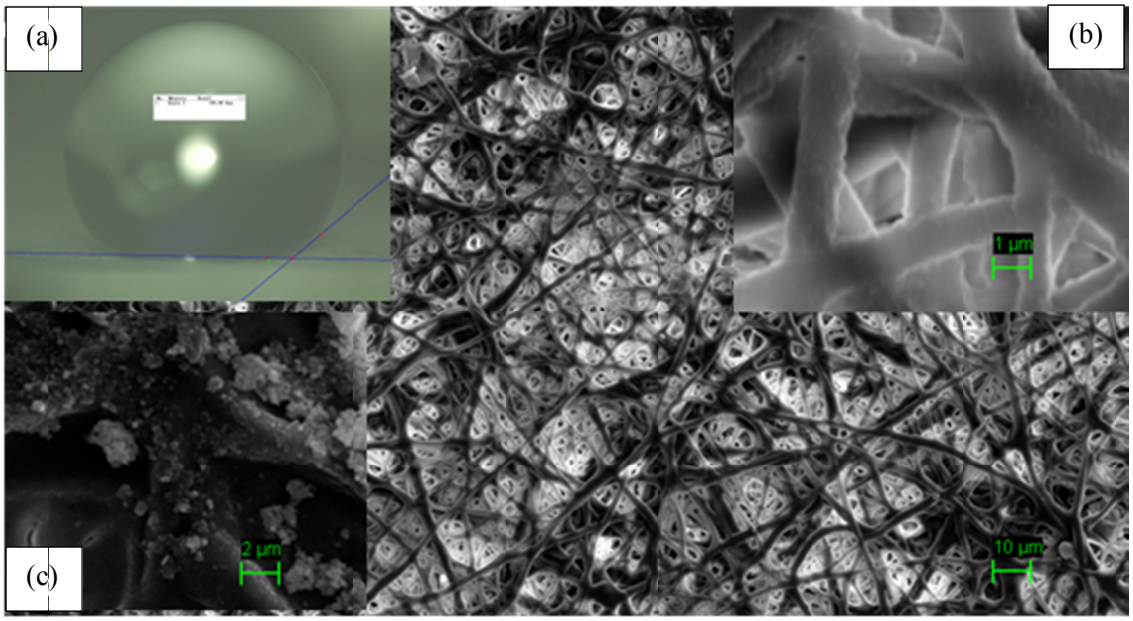

Figure 22: *Digital and SEM images of nanoparticle coated E344.*
(a) Water contact angle measurement, (b) enlarged SEM image showing coated fibre texture,
(c) center thick coated portion of the mat, (d) overall mat view.

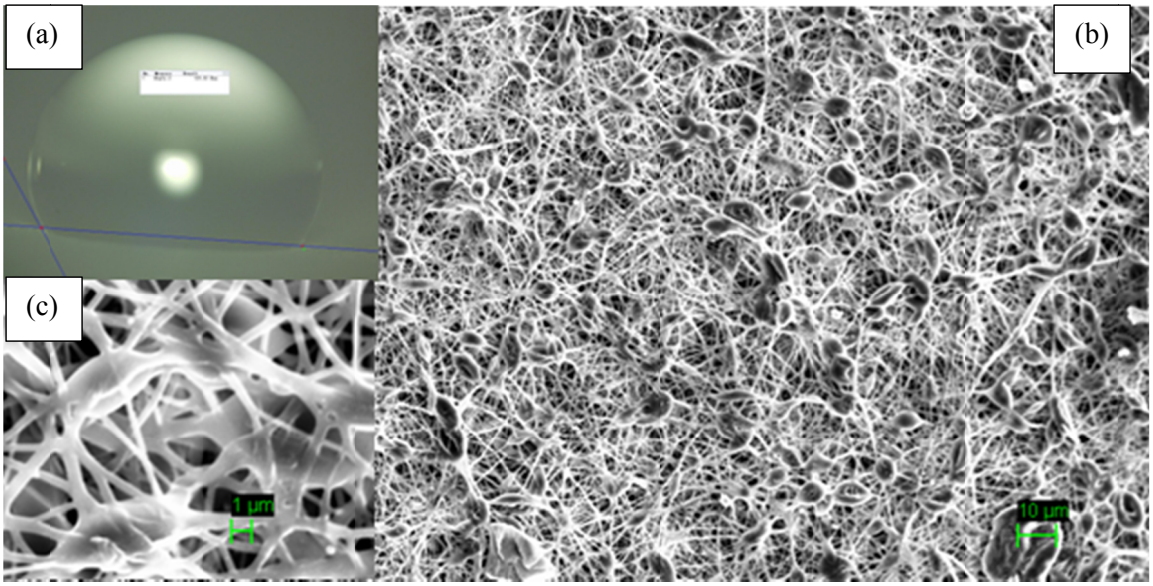

Figure 23: *SEM and microscope images of electrospun beaded fibre mat E384.*
(a) Water drop on the surface, (b) image of the uncoated surface,
and (c) enlargement of the beaded region showing fusing and small scale fibres.

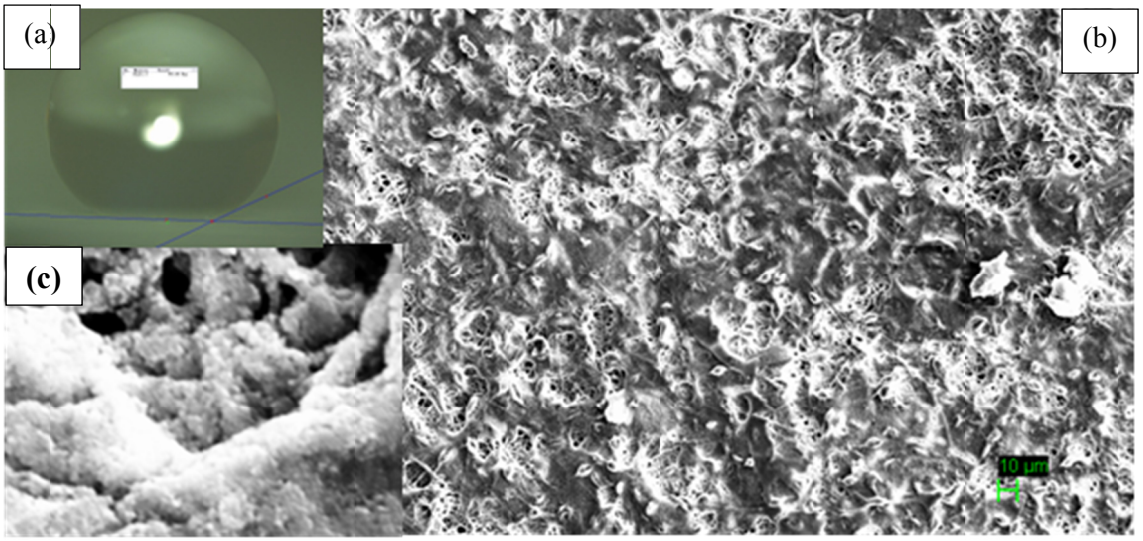

Figure 24: *SEM and microscope images of sol-gel coated electrospun beaded fibre mat E384.*
(a) Water drop on the coated surface, (b) image of the coated surface,
and (c) enlarged image of the beaded region showing fusing and small scale fibres.

4 Conclusions

This study has provided insights into the experimental conditions required for electrospinning polyurethane fibres. Polymer solution viscosity, flow rate, and the applied potential had an effect on the fibre diameter and the presence of beads. Smooth, large diameter fibres were formed for high viscosity polymer solutions, and high flow rates. Beading occurred for low viscosity solutions. Under the experimental conditions assessed, large needle-collector distances, low potential differences, low solution flow rates, and volatile solvents aided in the formation of unfused polymer fibres. Some of these parameters reduced the electrospinning rate. Long electrospinning times resulted in the production of dense fibre mats which were preferred for studying the materials hydrophobic properties.

The roughness of the mats was increased by producing beaded fibres, by the addition of nanoparticles to the polymer solution, and by sol-gel coating. Contact angle and tilt angle measurements of a spin coated polyurethane sample indicated that this polymer is hydrophilic. Contact angle measurements of the electrospun fibre mats showed an increase over the smooth polymer. This is attributed to the increase in surface roughness. Water drops on the uncoated fibre mats were metastable and were observed to collapse into a Wenzel state. Electrospun mats with titanium dioxide nanoparticles produced higher contact angles, though these materials were still hydrophilic and pinned water drops on the surface.

Hydrophobic sol-gel coatings of the textiles and the electrospun hydrophilic polyurethane, increased the contact angles considerably, and in a number of cases tilt angles were measured. Thick sol-gel coatings resulted in rougher surfaces and contact angles greater than 150^{o} and tilt angles less than 5^{o} were measured, thus demonstrating the ability to produce a superhydrophobic surface in the Cassie-Baxter state, from these materials.

As a final note, the surfaces studied here did not prove to be oleophobic, or oil repellent, though the sol-gel treated spin coated Pellethane on a glass slide did show some promise.

5 Future Work

The current work has laid a foundation of methods for producing electrospun fibres and an understanding of some of the major factors affecting fibre structure. Electrospun fibre mats have shown some promise as a superhydrophobic material with an increase in the contact angle over that of the smooth polymer. In addition this work has touched on two methods for increasing the fibre roughness and hydrophobicity, namely by incorporation of nanoparticles into the electrospinning solution and sol-gel coating of the fibres, which resulted in the achievement of a superhydrophobic surface. Indeed these studies have been by no means exhaustive, and there are a number of promising techniques for increasing surface roughness and decreasing the solid-liquid surface tension.

Methods to reduce the solid-liquid surface tension could be:

- Electrospinning solutions containing hydrophobic polymers;
- Adding hydrophobic nanoparticles to the electrospinning solution;
- Applying hydrophobic coatings; and
- Coating the surface by plasma polymerizing hydrophobic monomers.

Methods to increase the surface roughness include:

- Adding hydrophobic nanoparticles to the electrospinning solution;
- Adding nanoparticles in a coating;
- Electrospinning phase separating polymer mixtures;
- Grafting or polymerizing polymer chains onto the fibre surface; and
- Electrospinning a dilute polymer solution onto the fibre mat.

This page intentionally left blank.

References

[1] Li, X. M.; Reinhoudt, D.; Crego-Calama, M. *Chemical Society Reviews* (2007), *36*, 1529.

[2] Balu, B.; Breedveld, V.; Hess, D. W. *Langmuir* (2008), *24*, 4785.

[3] Yoon, Y. I.; Moon, H. S.; Lyoo, W. S.; Lee, T. S.; Park, W. H. *Carbohydrate Polymers* (2009), *75*, 246.

[4] Crowe, J. A.; Efimenko, K.; Genzer, J. In *ACS Symposium Series* (2007); Vol. 964, p 222.

[5] Shi, F.; Wang, Z. Q.; Zhang, X. *Advanced Materials* (2005), *17*, 1005.

[6] Li, J.; Fu, J.; Cong, Y.; Wu, Y.; Xue, L. J.; Han, Y. C. *Applied Surface Science* (2006), *252*, 2229.

[7] Dong, H. J.; Brook, M. A.; Brennan, J. D. *Chemistry of Materials* (2005), *17*, 2807.

[8] Doshi, D. A.; Shah, P. B.; Singh, S.; Branson, E. D.; Malanoski, A. P.; Watkins, E. B.; Majewski, J.; van Swol, F.; Brinker, C. J. *Langmuir* (2005), *21*, 7805.

[9] Rao, A. V.; Kulkarni, M. M.; Amalnerkar, D. P.; Seth, T. *J. Non-Cryst. Solids* (2003), *330*, 187.

[10] Shirtcliffe, N. J.; McHale, G.; Newton, M. I.; Perry, C. C. *Langmuir* (2003), *19*, 5626.

[11] Shirtcliffe, N. J.; McHale, G.; Newton, M. I.; Perry, C. C.; Roach, P. *Chemical Communications* (2005), 3135.

[12] Ma, M.; Gupta, M.; Li, Z.; Zhai, L.; Gleason, K. K.; Cohen, R. E.; Rubner, M. F.; Rutledge, G. C. *Advanced Materials* (2007), *19*, 255.

[13] Ma, M.; Hill, R. M.; Lowery, J. L.; Fridrikh, S. V.; Rutledge, G. C. *Langmuir* (2005), *21*, 5549.

[14] Ma, M. L.; Mao, Y.; Gupta, M.; Gleason, K. K.; Rutledge, G. C. *Macromolecules (*2005), *38*, 9742.

[15] Beckford, S.; Langston, N.; Zou, M.; Wei, R. *Applied Surface Science* (2011), *257*, 5688.

[16] Wang, C.-H.; Sun, D.-C.; Xia, X.-H. *Nanotechnology* (2006), *17*, 651.

[17] Wang, H. X.; Fang, J.; Cheng, T.; Ding, J.; Qu, L. T.; Dai, L. M.; Wang, X. G.; Lin, T. *Chemical Communications* (2008), 877.

[18] Huang, Z.-M.; Zhang, Y. Z.; Kotaki, M.; Ramakrishna, S. *Composites Science and Technology* (2003), *63*, 2223.

[19] Teo, W. E.; Ramakrishna, S. *Nanotechnology* (2006), *17*, R89.

[20] Acatay, K.; Simsek, E.; Ow-Yang, C.; Menceloglu, Y. Z. *Angewandte Chemie - International Edition* (2004), *43*, 5210.

[21] Drew, C.; Wang, X.; Samuelson, L. A.; Kumar, J. *Journal of Macromolecular Science, Part A* (2003), *40*, 1415.

[22] Agarwal, S.; Horst, S.; Bognitzki, M. *Macromol. Mater. Eng.* (2006), *291*, 592.

[23] Mahltig, B.; Haufe, H.; Bottcher, H. *Journal of Materials Chemistry* (2005), *15*, 4385.

[24] Wang, H.; Fang, J.; Cheng, T.; Ding, J.; Qu, L.; Dai, L.; Wang, X.; Lin, T. *Chemical Communications* (2008), 877.

[25] LSU Molecular Studies Group, Common Solvent Properties, http://macro.lsu.edu/HowTo/solvents.htm, (Accessed 06/01/2015).

Annex A Sol-gel coated fibres

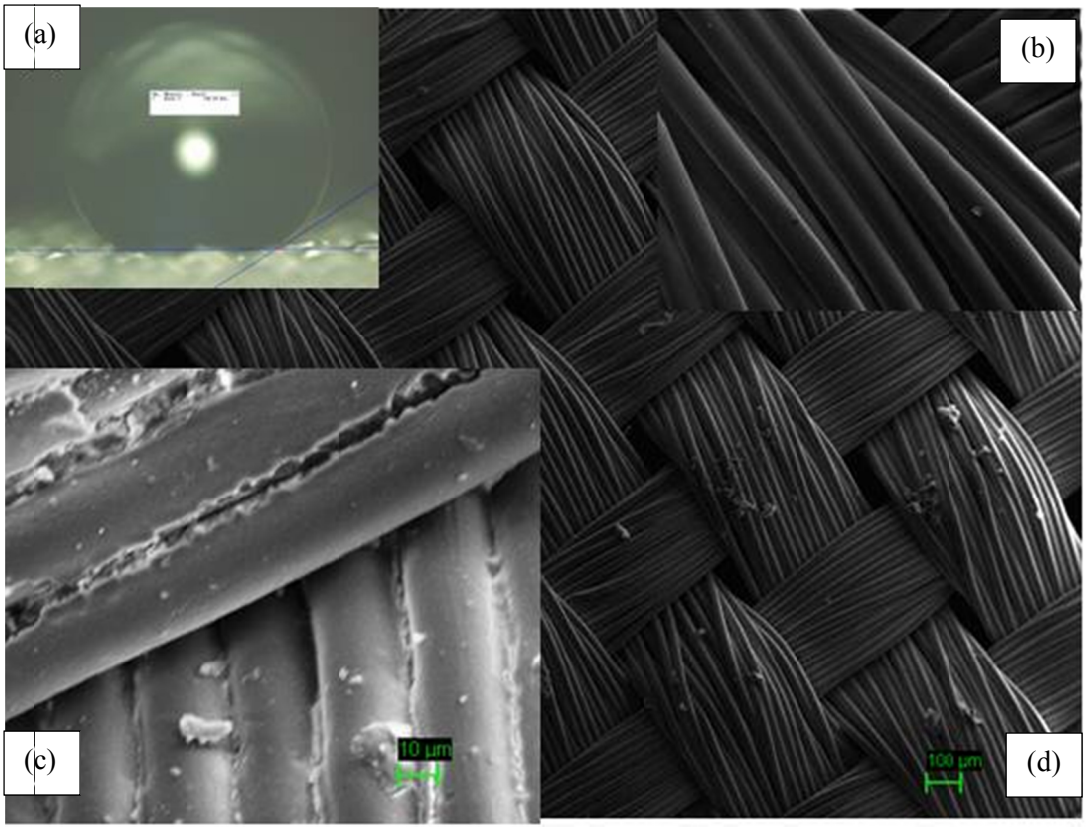

Figure A.1: *SEM and microscope images of a thick PET sample.*
(a) Contact angle measurement using 5 µL of water on the sol-gel coated textile,
(b) and (c) SEM images of the PET fabric pre and post sol-gel coating,
and (d) larger area view of textile.

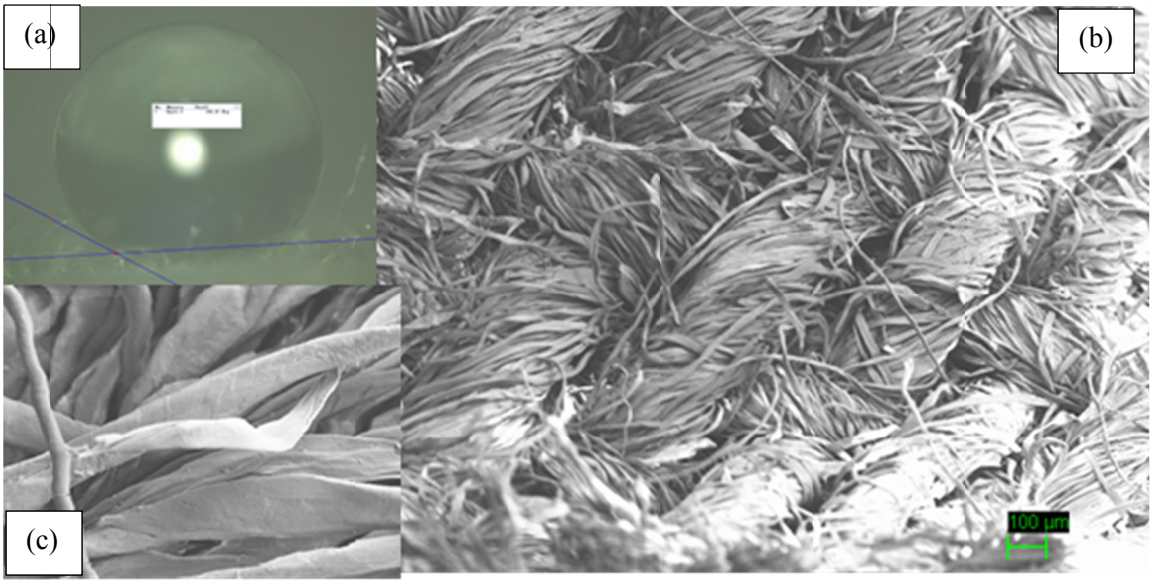

Figure A.2: *SEM and microscope images of a cotton textile.*
(a) Water drop on textile, (b) cotton textile, and (c) enlargement of cotton fibres.

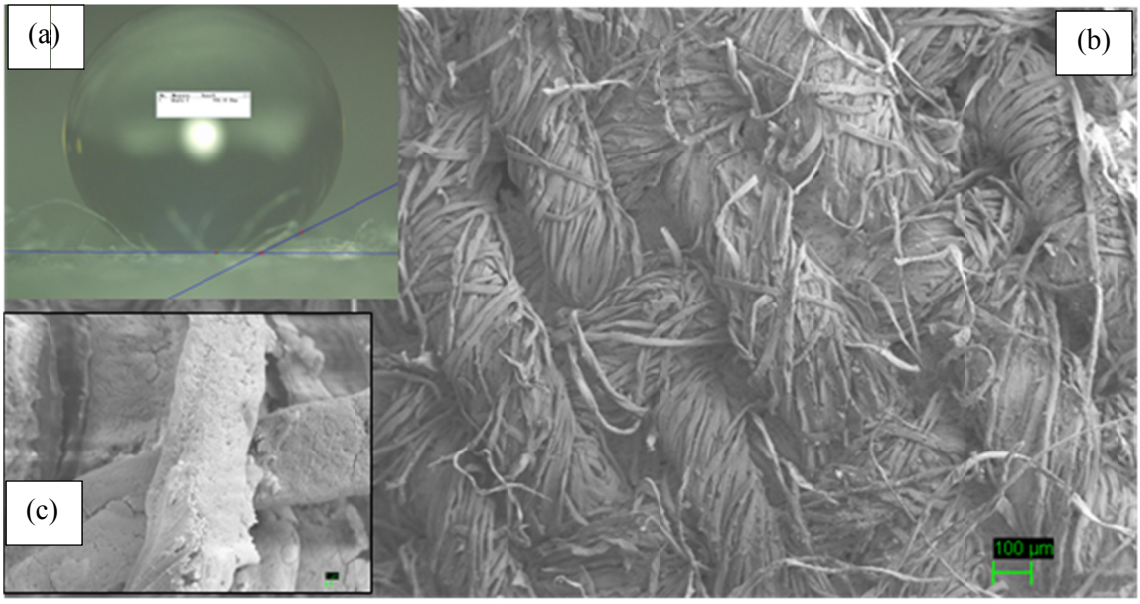

Figure A.3: *SEM and microscope images of cotton textile after sol-gel coating.*
(a) Water drop on sol-gel coated textile, (b) cotton textile,
and (c) enlargement of treated cotton fibres.

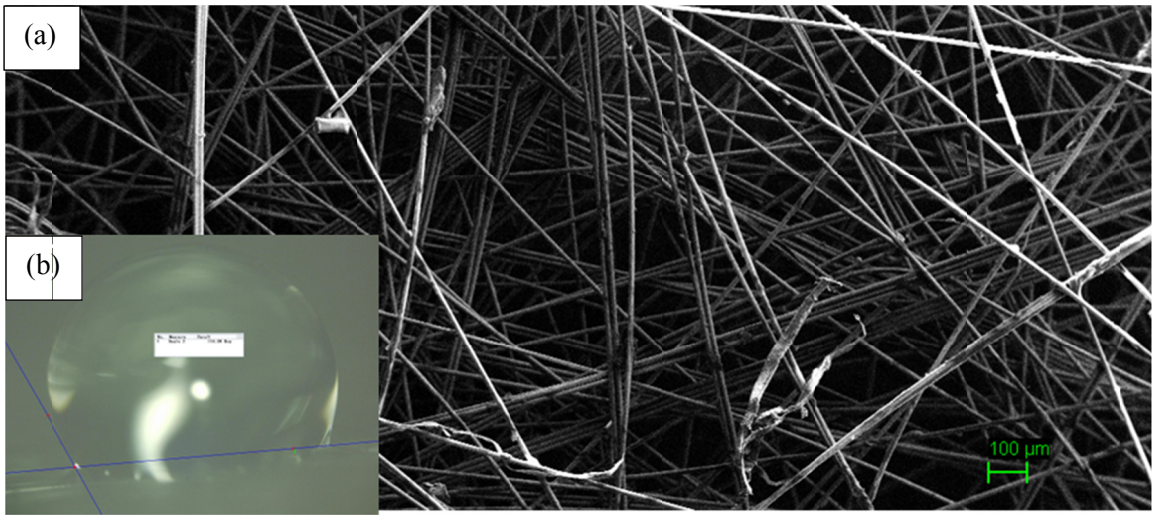

Figure A.4: *Glass Fibre Mesh SEM and Digital Microscope images.*
(a) Water contact angle measurement using Keyence Microscope,
(b) SEM image of the glass fibres making up the mesh/fabric.

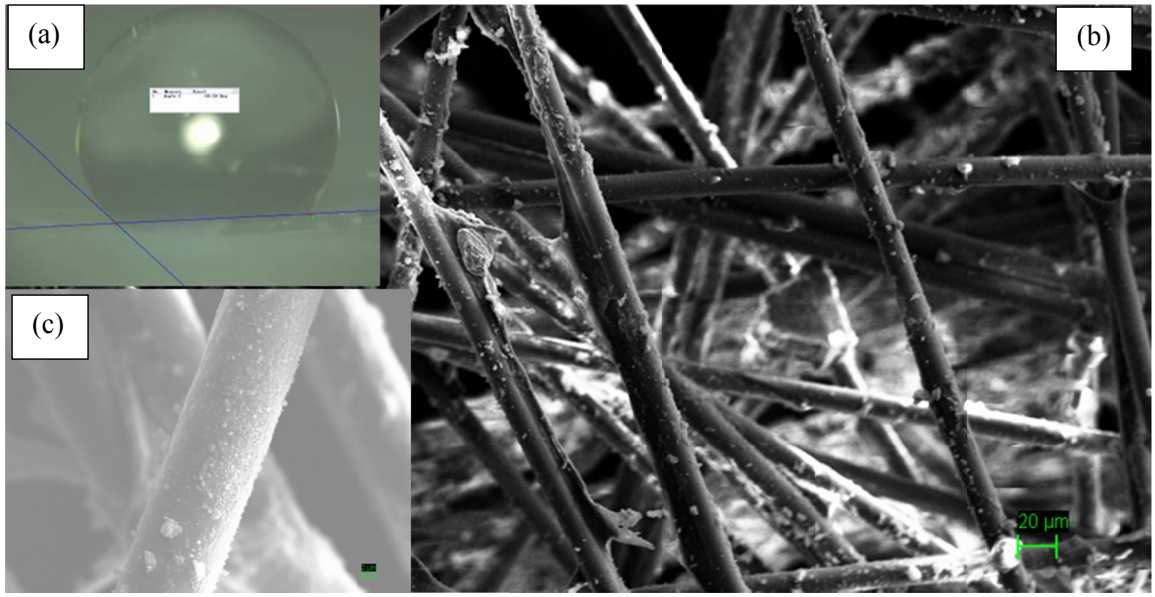

Figure A.5: *SEM and Digital Microscope images of Coated Glass fibre mesh.*
(a) Water contact angle measurement, (b) SEM image of overall fibre appearance,
(c) enlarged fibre image to show surface texture of the coated fibres.

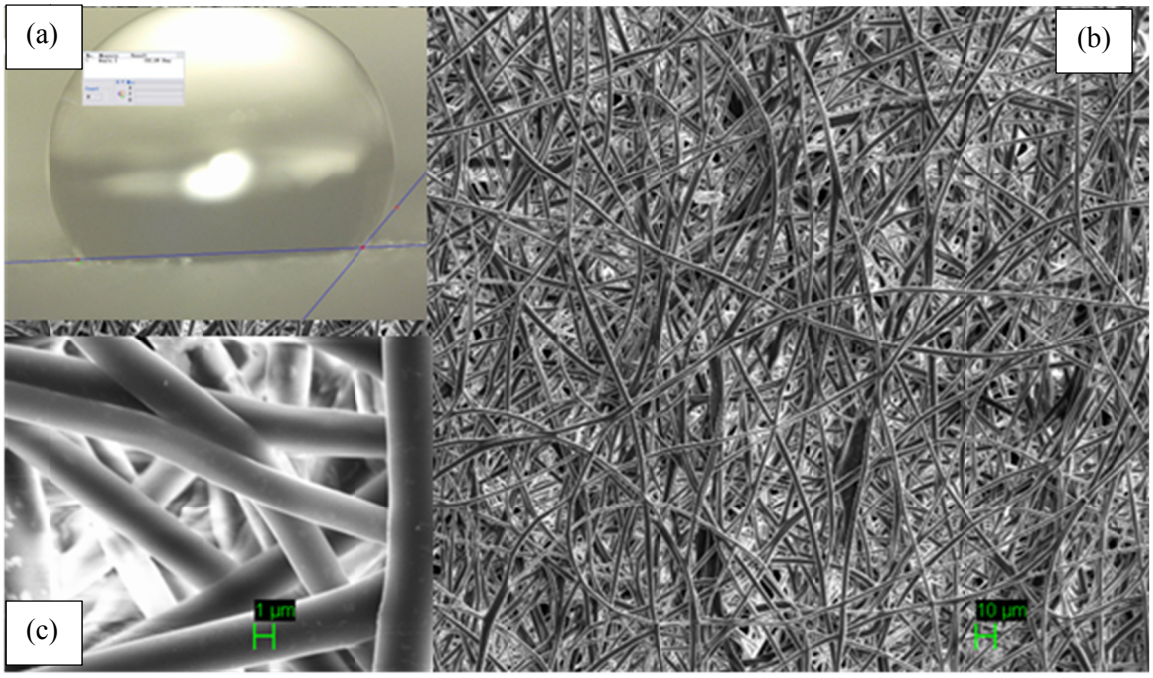

Figure A.6: *SEM and Digital Microscope Images of uncoated E 371.*
(a) Water contact angle measurement, (b) SEM image of electrospun fibre mat,
(c) enlarged SEM image showing the fibres' texture.

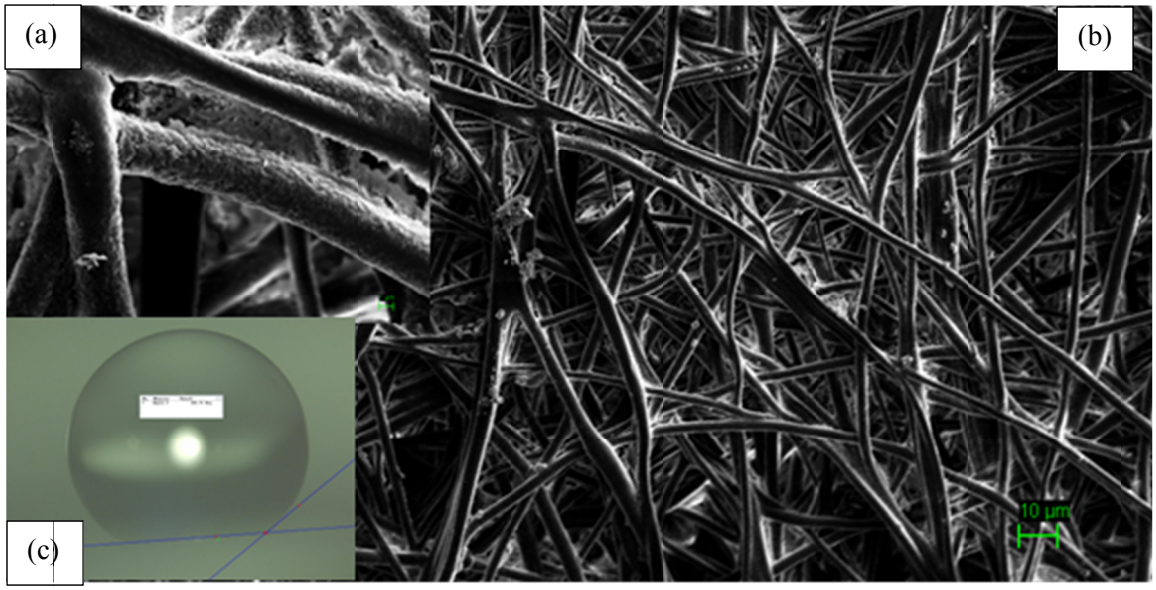

Figure A.7: *SEM and Digital Microscope Images of Nanoparticle coated E 371.*
(a) Enlarged SEM image showing the fibres' texture, (b) SEM image of electrospun fibre mat,
(c) water contact angle measurement.

List of symbols/abbreviations/acronyms/initialisms

DMF	N,N'-dimethyl formamide
DND	Department of National Defence
DRDC	Defence Research and Development Canada
DSTKIM	Director Science and Technology Knowledge and Information Management
FAS	tridecafluorooctyl triethoxy Silane
PET	polyethylene teraphthalate
R&D	Research & Development
SEM	Scanning Electron Microscope
TEOS	tetraethoxy orthosilicate
THF	tetrahydrofuran

This page intentionally left blank.

DOCUMENT CONTROL DATA

(Security markings for the title, abstract and indexing annotation must be entered when the document is Classified or Designated)

1. ORIGINATOR (The name and address of the organization preparing the document. Organizations for whom the document was prepared, e.g., Centre sponsoring a contractor's report, or tasking agency, are entered in Section 8.)

DRDC – Atlantic Research Centre
Defence Research and Development Canada
9 Grove Street
P.O. Box 1012
Dartmouth, Nova Scotia B2Y 3Z7
Canada

2a. SECURITY MARKING (Overall security marking of the document including special supplemental markings if applicable.)

UNCLASSIFIED

2b. CONTROLLED GOODS

(NON-CONTROLLED GOODS)
DMC A
REVIEW: GCEC APRIL 2011

3. TITLE (The complete document title as indicated on the title page. Its classification should be indicated by the appropriate abbreviation (S, C or U) in parentheses after the title.)

Electrospinning and Superhydrophobic Materials

4. AUTHORS (last name, followed by initials – ranks, titles, etc., not to be used)

Klein, P.; Kaye, B.J.; Saville, P.

5. DATE OF PUBLICATION (Month and year of publication of document.)	6a. NO. OF PAGES (Total containing information, including Annexes, Appendices, etc.)	6b. NO. OF REFS (Total cited in document.)
April 2015	42	25

7. DESCRIPTIVE NOTES (The category of the document, e.g., technical report, technical note or memorandum. If appropriate, enter the type of report, e.g., interim, progress, summary, annual or final. Give the inclusive dates when a specific reporting period is covered.)

Scientific Report

8. SPONSORING ACTIVITY (The name of the department project office or laboratory sponsoring the research and development – include address.)

DRDC – Atlantic Research Centre
Defence Research and Development Canada
9 Grove Street
P.O. Box 1012
Dartmouth, Nova Scotia B2Y 3Z7
Canada

9a. PROJECT OR GRANT NO. (If appropriate, the applicable research and development project or grant number under which the document was written. Please specify whether project or grant.)	9b. CONTRACT NO. (If appropriate, the applicable number under which the document was written.)
12sz20	

10a. ORIGINATOR'S DOCUMENT NUMBER (The official document number by which the document is identified by the originating activity. This number must be unique to this document.)	10b. OTHER DOCUMENT NO(s). (Any other numbers which may be assigned this document either by the originator or by the sponsor.)
DRDC-RDDC-2015-R049	

11. DOCUMENT AVAILABILITY (Any limitations on further dissemination of the document, other than those imposed by security classification.)

Unlimited

12. DOCUMENT ANNOUNCEMENT (Any limitation to the bibliographic announcement of this document. This will normally correspond to the Document Availability (11). However, where further distribution (beyond the audience specified in (11) is possible, a wider announcement audience may be selected.))

Unlimited

13. ABSTRACT (A brief and factual summary of the document. It may also appear elsewhere in the body of the document itself. It is highly desirable that the abstract of classified documents be unclassified. Each paragraph of the abstract shall begin with an indication of the security classification of the information in the paragraph (unless the document itself is unclassified) represented as (S), (C), (R), or (U). It is not necessary to include here abstracts in both official languages unless the text is bilingual.)

Many processes are affected by the interaction of liquids with surfaces. These interactions depend on the solid-liquid, solid-vapour, and liquid-vapour surface tensions, as well as the surface structure or roughness. A liquid in intimate contact with a rough surface will generally be better adhered than the same liquid on a smooth surface due to the increase in the contact area. Rough superhydrophobic surfaces with low surface energy, however, support the liquid on the peaks of the roughness, with minimal contact area, and as a consequence the liquid is easily removed. In this work durable micron sized polyurethane fibres were produced by electrospinning. The surface of these fibre mats was microscopically rough, and nano-scale features were added to the fibre surface by electrospinning with nanoparticles, or through a fluorinated alkyl silane, sol-gel coating process. The sol-gel treatment produced a rough hydrophobic coating on the electrospun fibres. From contact angle measurements, it was found that these methods increased the water contact angle, however, a truly superhydrophobic surface with small tilt angle was only achieved when a thicker sol-gel coating was deposited on the electrospun fibre mats.

De nombreux processus sont affectés par l'interaction des liquides avec les surfaces. Ces interactions dépendent des tensions superficielles solide-liquide, solide-vapeur et liquide-vapeur, ainsi que de la structure de la surface et de sa rugosité. Un liquide en contact étroit avec une surface rugueuse y adhèrera généralement mieux que sur une surface lisse en raison de la surface de contact plus grande. Toutefois, les surfaces rugueuses superhydrophobes à faible énergie superficielle supportent le liquide sur leurs parties les plus rugueuses, là où le contact est minimal, et, en conséquence, le liquide facilement extrait. Pour le présent travail, nous avons produit des fibres de polyuréthane durable de la taille de l'ordre du micron par électrofilage. La surface de ces mats fibreux était rugueuse au microscope et des caractéristiques à l'échelle nanométrique ont été ajoutées à la surface des fibres par électrofilage au moyen de nanoparticules ou grâce à un procédé de revêtement sol-gel avec un alkylsilane fluoré. Le traitement par sol-gel a produit un revêtement rugueux hydrophobe sur les fibres électrofilées. À partir de mesures d'angles de contact, nous avons montré que ces méthodes accroissaient l'angle de contact de l'eau. Toutefois, seule une surface vraiment superhydrophobe avec un petit angle d'inclinaison a pu être obtenue quand un revêtement sol-gel plus épais était déposé sur les mats fibreux électrofilés.

14. KEYWORDS, DESCRIPTORS or IDENTIFIERS (Technically meaningful terms or short phrases that characterize a document and could be helpful in cataloguing the document. They should be selected so that no security classification is required. Identifiers, such as equipment model designation, trade name, military project code name, geographic location may also be included. If possible keywords should be selected from a published thesaurus, e.g., Thesaurus of Engineering and Scientific Terms (TEST) and that thesaurus identified. If it is not possible to select indexing terms which are Unclassified, the classification of each should be indicated as with the title.)

Superhydrophobic; Electrospinning; Polymer; Fibre; Contact Angle; Nanoparticles; Sol-Gel